

LOCKHEED MARTIN ENERGY RESEARCH LIBRARIES



3 4456 0515616 7

CENTRAL RESEARCH LIBRARY

ORNL-4932

cy. 1

ORNL ISOTOPIC POWER FUELS
QUARTERLY REPORT
FOR PERIOD ENDING SEPTEMBER 30, 1973

Eugene Lamb

OAK RIDGE NATIONAL LABORATORY
CENTRAL RESEARCH LIBRARY
DOCUMENT COLLECTION

LIBRARY LOAN COPY

DO NOT TRANSFER TO ANOTHER PERSON

If you wish someone else to see this
document, send in name with document
and the library will arrange a loan.

UCN-7969
(3 3-67)



OAK RIDGE NATIONAL LABORATORY

OPERATED BY UNION CARBIDE CORPORATION • FOR THE U.S. ATOMIC ENERGY COMMISSION

Printed in the United States of America. Available from
National Technical Information Service
U.S. Department of Commerce
5285 Port Royal Road, Springfield, Virginia 22151
Price: Printed Copy \$5.45; Microfiche \$1.45

This report was prepared as an account of work sponsored by the United States Government. Neither the United States nor the United States Atomic Energy Commission, nor any of their employees, nor any of their contractors, subcontractors, or their employees, makes any warranty, express or implied, or assumes any legal liability or responsibility for the accuracy, completeness or usefulness of any information, apparatus, product or process disclosed, or represents that its use would not infringe privately owned rights.

ORNL-4932
UC-33 -- Nuclear Propulsion
Systems and Aerospace Safety

Contract No. W-7405-eng-26

ISOTOPES DEVELOPMENT CENTER

ORNL ISOTOPIC POWER FUELS QUARTERLY REPORT
FOR PERIOD ENDING SEPTEMBER 30, 1973

Eugene Lamb

Isotopes Division

DECEMBER 1973

OAK RIDGE NATIONAL LABORATORY
Oak Ridge, Tennessee 37830
operated by
UNION CARBIDE CORPORATION
for the
U.S. ATOMIC ENERGY COMMISSION



3 4456 0515616 7



CONTENTS

	<u>Page</u>
SUMMARY	1
CURIUM-244 FUEL DEVELOPMENT	2
²⁴⁴ Cm ₂ O ₃ Compatibility Program	2
Compatibility Couple Tests	2
Cm ₂ O ₃ Source Test Capsule	4
Cm ₂ O ₃ Compatibility With Ceramic Materials	5
FY 1974 Compatibility Matrix	9
Reaction of Cm ₂ O ₃ With Pt-26% Rh-8% W Alloy	9
Reaction of Cm ₂ O ₃ With T-111 Alloy	10
Reaction of Cm ₂ O ₃ With Hafnalloy 20-20	14
Reaction of Cm ₂ O ₃ With Stainless Steel 316 Alloy	16
Reaction of Cm ₂ O ₃ With Ir-2% W Alloy	18
Reaction of Cm ₂ O ₃ With Pt-30% Rh-8% W Alloy	20
Reaction of Cm ₂ O ₃ With Carbon	21
²⁴⁴ Cm ₂ O ₃ Property Characterization	23
Helium Release	23
Vapor Pressure	23
X-Ray Diffraction	23
Emissivity	24
Heat Capacity	24
Dimensional Stability	25
Rate of Dissolution of Cm ₂ O ₃ in Seawater	26
Reaction of Cm ₂ O ₃ With Dry Air	29
²⁴⁴ Cm ₂ O ₃ Radiation Measurements	30
Impact Testing of Heat Source Materials	32
Assay of SRL-31 Curium-244 Oxide	32
Curium Oxide Purification	34
Curium From Power Reactor Fuels	37
Curium Source Fabrication Facility Operation	41
REFERENCES	42

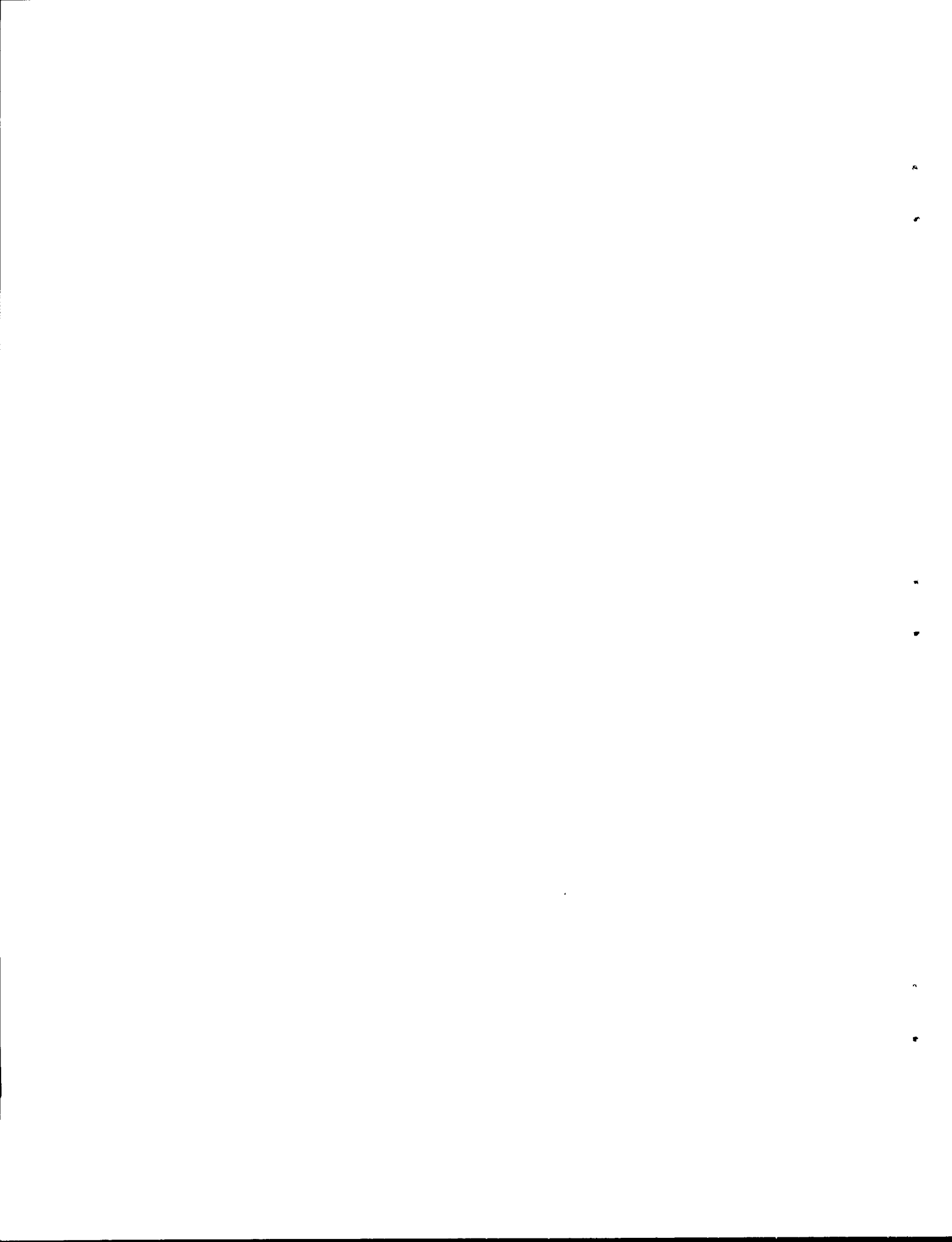
LIST OF FIGURES

Fig. 1. Cross-Sectional View of Bottom of Curium Kilowatt Source Capsule	6
Fig. 2. Curium Kilowatt Source Capsule, Vent Disc and Vent Tube	7
Fig. 3. Rate of Loss of ²⁴⁴ Cm From Surface of Pellet in Seawater	28
Fig. 4. Oxidation of Cm ₂ O ₃ Exposed to Dry Air	30
Fig. 5. Influence of Enrichment on Curium Production	39

LIST OF TABLES

	<u>Page</u>
Table 1. Status of Compatibility Tests	3
Table 2. Oxygen Analysis of Compatibility Samples	4
Table 3. $^{244}\text{Cm}_2\text{O}_3$ Ceramic Compatibility Experiments	5
Table 4. Partial Molar Free Energies of Mixing of Components in Pt-26% Rh-8% W	10
Table 5. Gibbs Free Energy of Formation of Pt_3O_4 , WO_2 , Rh_2O , PuO_2 , and Pu_2O_3	11
Table 6. Gibbs Free Energies of Reaction for Eqs. 2-5	12
Table 7. Partial Molar Free Energies of Mixing of Components in T-111	12
Table 8. Gibbs Free Energy of Formation of Ta_2O_5 , WO_2 , HfO_2 , PuO_2 , and Pu_2O_3	13
Table 9. Gibbs Free Energies of Reaction for Eqs. 6-11	13
Table 10. Partial Molar Free Energies of Mixing of Components in Hafnalloy 20-20	14
Table 11. Gibbs Free Energies of Formation of HfO_2 , SnO_2 , PdO , Pt_3O_4 , PuO_2 , and Pu_2O_3	15
Table 12. Gibbs Free Energies of Reaction for Eqs. 12-17	15
Table 13. Partial Molar Free Energies of Mixing of Elements in Stainless Steel 316	16
Table 14. Gibbs Free Energies of Formation of Fe_3O_4 , Cr_2O_3 , NiO , MnO , SiO_2 , MoO_2 , PuO_2 , and Pu_2O_3	16
Table 15. Gibbs Free Energies of Reaction for Eqs. 18, 20, 22, 24, 26, and 28	17
Table 16. Gibbs Free Energies of Reaction for Eqs. 19, 21, 23, 25, 27, and 29	18
Table 17. Partial Molar Free Energies of Mixing of Components of Ir-2% W Alloy	18
Table 18. Gibbs Free Energies of Formation of Ir_2O_3 , WO_2 , Pu_2O_3 , and PuO_2	19
Table 19. Gibbs Free Energies of Reaction for Eqs. 30-33	19

	<u>Page</u>
Table 20. Partial Molar Free Energies of Mixing of Components of Pt-30% Rh-8% W	20
Table 21. Gibbs Free Energy of Formation of Pt ₃ O ₄ , Rh ₃ O, WO ₃ , Pu ₂ O ₃ , and PuO ₂	20
Table 22. Gibbs Free Energies of Reaction for Eqs. 34-37	21
Table 23. Gibbs Free Energies of Reaction of Cm ₂ O ₃ With Carbon to Produce Cm, CmC _{0.5} O _{0.5} , CmC _{0.9} , CmC _{1.5} , and CmC ₂	22
Table 24. Gibbs Free Energies of Reaction of Carbon With PuO ₂ to Produce Pu, PuO _{0.5} O _{0.5} , PuC _{0.9} , PuC _{1.5} , and PuC ₂	22
Table 25. Average ²⁴⁴ Cm ₂ O ₃ Pellet Densities	26
Table 26. Dissolution of Cm ₂ O ₃ in Boiling Seawater	29
Table 27. Neutron Spectra Data for ²⁴⁴ Cm ₂ O ₃	31
Table 28. Comparison of ORNL and SRL ²⁴⁴ Cm ₂ O ₃ Neutron Emissions Data	32
Table 29. Isotopic Abundances of Curium and Plutonium in SRL-31 Oxide	32
Table 30. Curium and Plutonium Content in SRL-31 Oxide	33
Table 31. Radioactive Impurities in SRL-31 Oxide	33
Table 32. Impurities in Batch SRL-31 Curium Oxide	34
Table 33. Curium Oxide Product Weight and ²⁴⁴ Cm Content	35
Table 34. Isotopic Analysis of Composite SR Cm-30, -31, -32	35
Table 35. Impurities in Composite SR Cm-30, -31, -32	35
Table 36. Curium Oxide Product Weight and ²⁴⁴ Cm Content	36
Table 37. Isotopic Analysis of Composite SR Cm-33, -34	36
Table 38. Impurities in Composite SR Cm-33, -34	36
Table 39. Average Neutron Flux as a Function of Fuel Enrichment	38
Table 40. Influence of ²³⁵ U Enrichment on ²⁴⁴ Cm Yield in Power Reactor Fuel	38
Table 41. Isotopic Abundance of Curium Isotopes for Various Power Reactor Fuels	41



ORNL ISOTOPIC POWER FUELS QUARTERLY REPORT
FOR PERIOD ENDING SEPTEMBER 30, 1973

Eugene Lamb

SUMMARY

Heat soak periods were completed on four of the ten sets of compatibility couples which were put on test during the previous quarter. The four sets contain a total of 18 couples. Four couples were examined, and tests on the others are in progress. Examination of the Kilowatt Test Source capsule was completed. Four Cm_2O_3 /ceramic couples were examined and additional tests are underway. Materials selection and test conditions were finalized for a 15-couple matrix to be initiated during FY 1974.

Free energy calculations were made for the reactions of Cm_2O_3 with Pt-26% Rh-8% W, T-111, Hafn alloy 20-20, stainless steel type 316, Ir-2% W, Pt-30% Rh-8% W, and carbon.

The equipment assemblies for the helium release, emissivity, vapor pressure, and heat capacity experiments were completed and checked out. Installation of the equipment for x-ray diffraction was completed, and the system was put into operation. Two x-ray diffraction examinations were made of pellets used for leach-rate studies.

A comparison of physical stability was made between two essentially identical Cm_2O_3 pellets, one stored in dry air and one stored in argon. Some degradation of the air-stored pellet was noted but there was no observable change in the pellet stored in argon. A significant variation in as-pressed density was observed between two Cm_2O_3 pellets prepared from materials of different ages using identical pressing conditions.

Measurements of rate-of-loss of ^{244}Cm from $^{244}\text{Cm}_2\text{O}_3$ pellets in seawater were made under two sets of conditions - fresh air-saturated flowing seawater at ambient temperature and a fixed volume of boiling seawater.

The rate of weight gain in dry air was measured for a hot-pressed Cm_2O_3 pellet of relatively low density. Calcination weight loss measurements and dry air weight gain measurements were made on a fraction of purified curium oxide.

Neutron radiation data from the ^{244}Cm source measurement made last quarter were analyzed and compared to literature values. The source was re-analyzed by calorimetry,

and the ^{244}Cm content as of date of the radiation measurement was calculated. A recheck of the low-energy range of the neutron spectra was initiated.

The equipment for the Cm_2O_3 impact study was stored due to a postponement of this project.

Analytical work on the ^{244}Cm product which is currently being used for characterization tests was completed. Two fractions of stored ^{244}Cm residues were processed at the TRU facility and yielded 77 g of highly pure curium oxide for test work.

Calculations of the yield of ^{244}Cm as a function of ^{235}U enrichment in PWR operations were made. The variation in isotopic abundances of the four principal curium isotopes were calculated for five reference reactors.

CURIUM-244 FUEL DEVELOPMENT

(Division of Space Nuclear Systems Program LR 30 01 03 3)

$^{244}\text{Cm}_2\text{O}_3$ Compatibility Program

Compatibility Couple Tests

(T. A. Butler and J. R. DiStefano)

The 1100°C compatibility couples contained in Sets 3, 4, 5, and 6 completed the scheduled heat soak periods on August 6 and August 9, 1973. The tantalum outer containers of Sets 3 and 5 were bulged due to internal pressure produced in the sealed helium atmosphere at the temperature of the test, but there was no evidence of rupture. The radiation readings of the combined neutron and gamma dose rates at a source-to-detector distance of about 3 in. was 850 mR/hr per gram of $^{244}\text{Cm}_2\text{O}_3$ fuel. The sets were transferred to HRLEL for metallographic examination.

The first power outage for Sets 1 and 2 occurred on September 12, 1973, and lasted for a period of 115 hr. The status of the 900, 1100, and 1400°C compatibility test matrix on September 27, 1973, is summarized in Table 1.

Visually, all of the 18 capsule assemblies from Sets 3, 4, 5, and 6 looked good upon removal from the capsule holders. Except for platinum, the top disc metal sample was removed for oxygen analysis. The platinum sample in each set appeared to be stuck and could not be easily removed. The capsule assemblies from Set 3 were vented to static helium and a graphite jacket surrounded the inner capsule. Metallographic observations can be summarized as follows:

Table 1. Status of Compatibility Tests

Set ^a	Start of Test	Thermal Cycles	Cumulative Hours	Projected End of Test
1	5-3-73	1	3413	12-3-73
2	5-3-73	1	3413	12-3-73
3	4-16-73	3	2560	8-6-73 ^b
4	4-16-73	3	2560	8-6-73 ^b
5	4-17-73	2	2510	8-9-73 ^b
6	4-17-73	2	2510	8-9-73 ^b
7	5-3-73	2	3416	12-3-73
8	5-3-73	2	3416	12-3-73
9	5-3-73	2	3408	12-3-73
10	5-3-73	2	3408	12-3-73

^aSet identifications:^bEnd

- 900°C; 5000 hr; helium atmosphere; Ir, C, Pt, Hf-1% Pt-0.5% Pd, Hastelloy C-276, Haynes 25, Haynes 188, ThO₂, Pt-20% Rh, and Pt-26% Rh-8% W.
- 900°C; 5000 hr; graphite, helium atmosphere; Ir, Pt, Hf-1% Pt-0.5% Pd, Hastelloy C-276, Haynes 25, Haynes 188, ThO₂, Pt-20% Rh, and Pt-26% Rh-8% W.
- 1100°C; 2500 hr; graphite, helium atmosphere; Ir, Pt, Pt₃Ir, and Pt-26% Rh-8% W-0.5% Ti.
- 1100°C; 2500 hr; dynamic vacuum; Ir, Pt, Pt₃Ir, C, and Pt-26% Rh-8% W-0.5% Ti.
- 1100°C; 2500 hr; helium atmosphere; Ir, Pt, Pt₃Ir, C, and Pt-26% Rh-8% W-0.5% Ti.
- 1100°C; 2500 hr; graphite, dynamic vacuum; Ir, Pt, Pt₃Ir, and Pt-26% Rh-8% W-0.5% Ti.
- 1400°C; 5000 hr; graphite, helium atmosphere; Ir, C, Mo, Mo-46% Re, Ta, T-111, W, and W-26% Re.
- 1400°C; 5000 hr; dynamic vacuum; Ir, Mo, Mo-46% Re, Ta, T-111, W, and W-26% Re.
- 1400°C; 5000 hr; helium atmosphere; Ir, Mo, Mo-46% Re, Ta, T-111, W, and W-26% Re.
- 1400°C; 5000 hr; graphite, dynamic vacuum; Ir, C, Mo, Mo-46% Re, Ta, T-111, W, and W-26% Re.

<u>Material</u>	<u>Remarks</u>
Platinum	Platinum samples and $^{244}\text{Cm}_2\text{O}_3$ reacted in certain locations to form Pt-Cm alloy or Pt-Cm-O compound.
Pt-26% Rh-8% W-0.5% Ti	Slight (1 mil) grain boundary attack of alloy.
Pt ₃ Ir	Slight surface roughening and grain boundary attack up to 1.5 mils in certain areas.
Iridium	Slight surface roughening.

Oxygen analyses from samples of the various materials (except platinum) from these tests are summarized in Table 2.

Table 2. Oxygen Analysis of Compatibility Samples

Material ^a	Oxygen Concentration (ppm)			
	Helium		Vacuum	
	Graphite ^b	Al ₂ O ₃ ^c	Graphite ^b	Al ₂ O ₃ ^c
Pt-26% Rh-8% W-0.5% Ti	107	61	23	79
Pt ₃ Ir	33	29	<10	<10
Iridium	<10	<10	<10	<10
Graphite		<10		<10

^a<10 ppm oxygen before test.

^bGraphite intermediate capsule and graphite capsule holder.

^cNo graphite intermediate capsule; Al₂O₃ capsule holder.

The relatively high oxygen pickup by Pt-26% Rh-8% W-0.5% Ti was probably caused by titanium, a strong oxide former. Note that Pt₃Ir vented to helium showed a slight pickup of oxygen while pure iridium did not. Since data for unalloyed platinum were not obtained, the reason for the pickup in Pt₃Ir is not clear. No significant effects of other variables such as the helium or vacuum environment or the graphite intermediate capsule on oxygen pickup were noted in the data we have obtained thus far.

Cm₂O₃ Source Test Capsule (*J. R. DiStefano*)

A vented tungsten capsule was used to contain Cm₂O₃ for over 660 days at temperatures from 1000-1400°C.¹ Some oxidation of the tungsten capsule occurred when the test system was disassembled. The Cm₂O₃ pellets were lodged tightly in each of the seven holes in which they were contained, and to permit handling and mounting of metallographic samples, most of the Cm₂O₃ had to be mechanically removed by drilling. It is possible that these procedures may have caused cracks in the tungsten capsule.

A cross-sectional view of one of the holes that contained some remaining Cm_2O_3 is shown in Fig. 1. There is considerable evidence of penetration of the tungsten by Cm_2O_3 , especially along grain boundaries. The tungsten also contains numerous cracks which were probably the result of cutting and drilling. The Cm_2O_3 contains some bright metallic particles which we believe to be tungsten. Attempts to analyze various phases in this specimen by microprobe analysis were unsuccessful because heat generated by the sample caused vaporization that rendered the optical and x-ray system inoperative.

Figure 2 shows a vent disc section and attached vent tube through which helium gas generated by decay of curium passed. Evidence of deposits are seen along surfaces of the vent disc, and the vent tube appears to be almost plugged. Microprobe analysis indicated the material in the vent tube plug to be a combination of curium oxide and tungsten oxide. The bright (white) phase in the deposit would seem to indicate the presence of metallic particles, but this is an artifact of polishing. Material deposited along the inside diameter of the vent tube is primarily tungsten oxide, while the bulk of the deposit is more a mixture of curium and tungsten oxides.

In summary, examination of the capsule from the source test indicates that under these conditions tungsten provided containment of Cm_2O_3 , but there was considerable grain boundary attack and mass transfer of tungsten. This makes unalloyed tungsten appear not to be a good choice for containment of Cm_2O_3 in the temperature range of 1200-1400°C and under conditions of a temperature gradient.

Cm_2O_3 Compatibility With Ceramic Materials (*P. Angelini*)

The plan of experiments is presented in Table 3.

Table 3. $^{244}\text{Cm}_2\text{O}_3$ Ceramic Compatibility Experiments

Experiment	Material	Temperature (°C)	Time (hr)
A	ThO_2	1500	24
B	ThO_2	1300	100
C	ThO_2	1500	500
D	ThO_2	1300	500
E	ZrO_2	1500	24
F	ZrO_2	1300	100
G	ZrO_2	1500	500
H	ZrO_2	1300	500
I	Al_2O_3	1500	500
J	Al_2O_3	1300	500

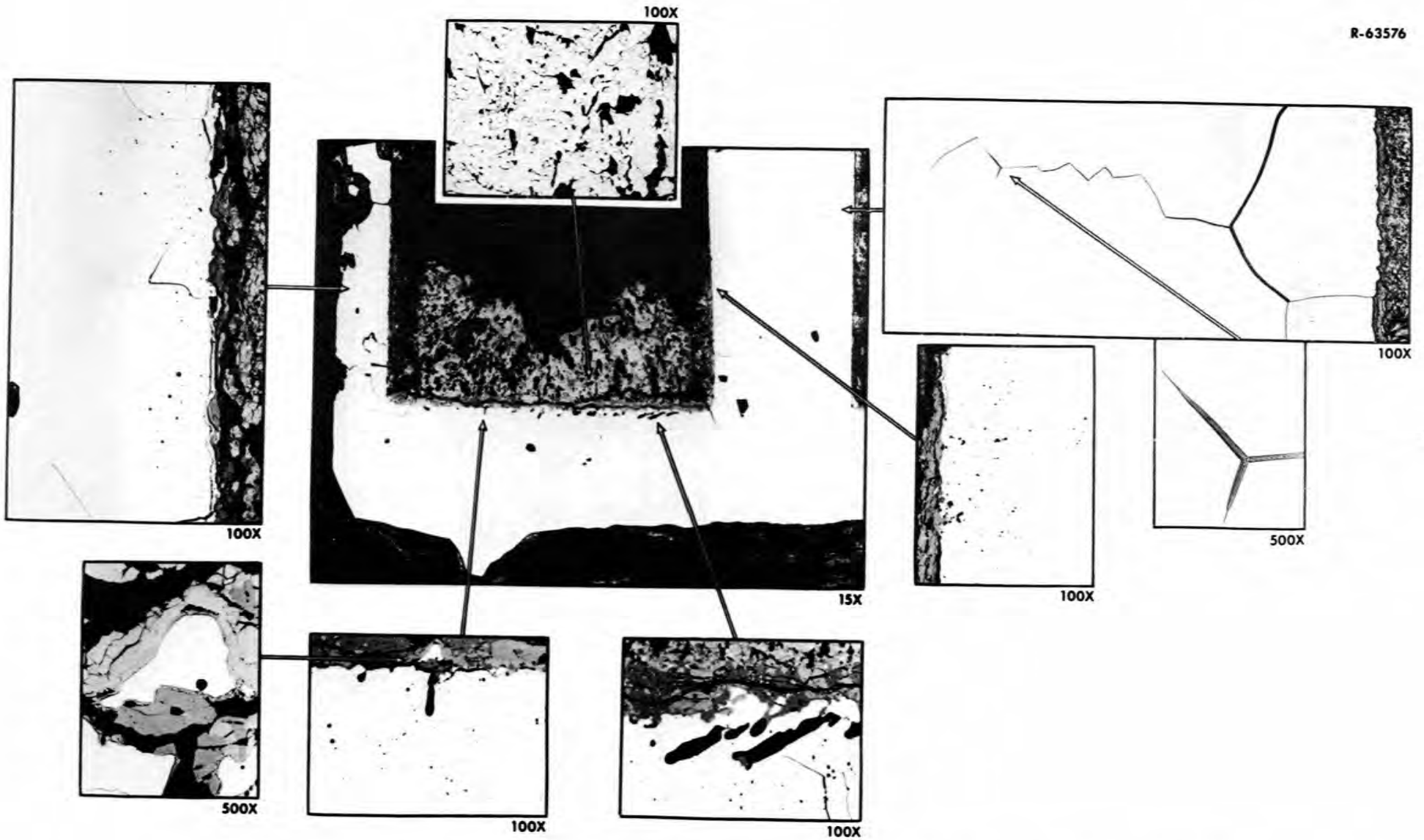


Fig. 1. Cross-Sectional View of Bottom of Curium Kilowatt Source Capsule.

R-63577

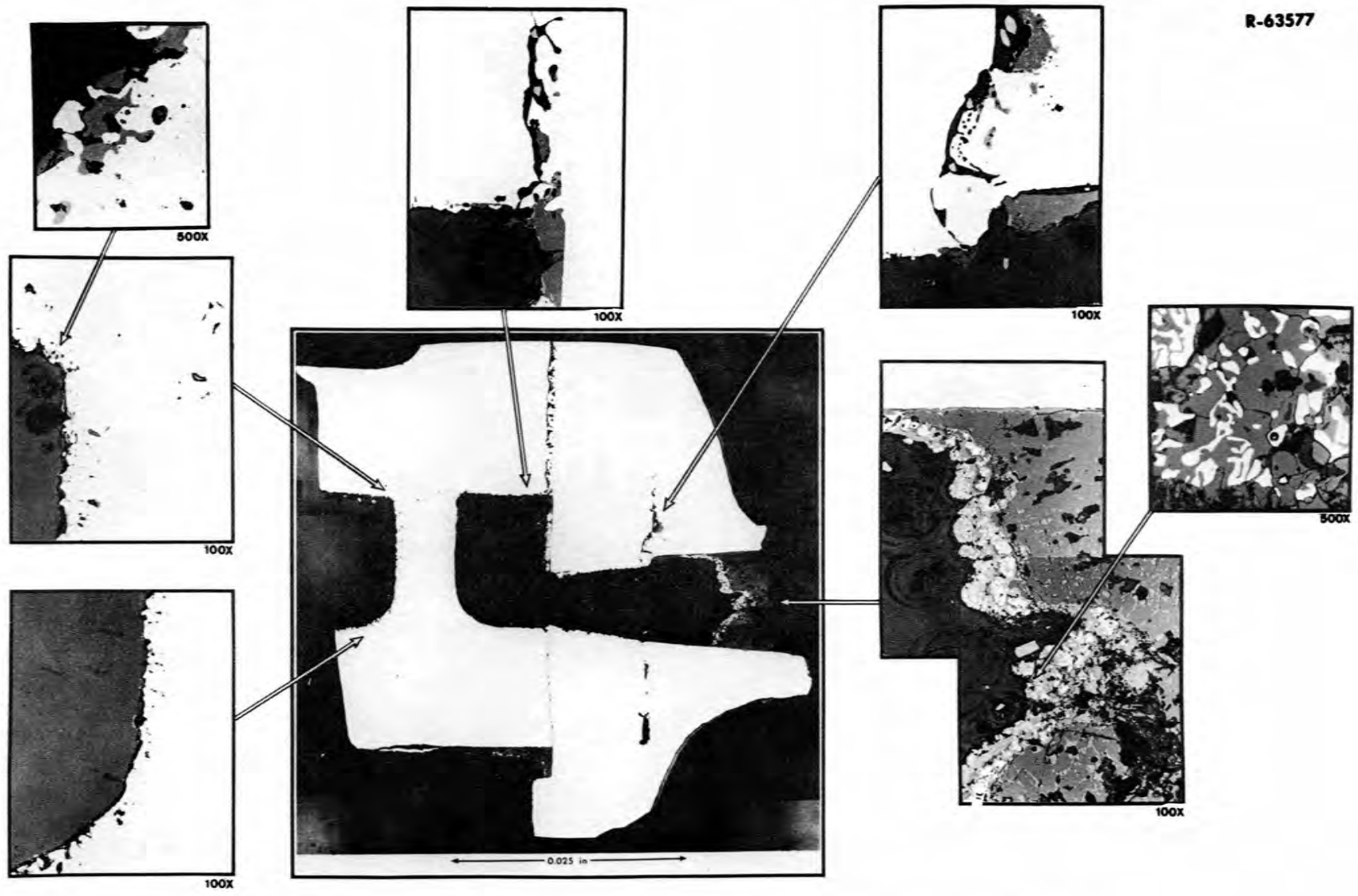


Fig. 2. Curium Kilowatt Source Capsule, Vent Disc and Vent Tube.

Optical microscopy on an as-fabricated 0.180-in.-diam pellet with a density of 10.2 g/cm^3 (from Savannah River powder batch SRL-31) has been completed. The pellet appeared very dense with very little porosity. The pellet had not changed shape and appeared to have the same dimensions as it had after fabrication; it had been exposed to air for over one month prior to examination.

To date, experiments A, B, E, and F have undergone their prescribed heating times. These couples have been mounted and polished, and the optical microscopy has been completed. The results obtained thus far do not show a great reaction between Cm_2O_3 and ThO_2 or ZrO_2 at either temperature. Unless the reactions occurring are very significant, it is difficult to determine quantitatively the extent of reaction by optical means in these cases.

The optical microscopy on the pellets in experiments A, B, E, and F showed that the fuel pellets had swelled and that the porosity had increased during their exposure at temperature. From the location and geometry of the voids, it is inferred that the helium generated and contained in the fuel during storage prior to the heating cycle was the cause of the expansion. The expansion is believed to have occurred during the initial heating period, at which time the bulk of the stored helium inventory escaped from the pellet. Both the diameter and height increased in dimension; however, the increase in height was not uniform across the pellet. This caused the pellets to lose much contact with the oxide inserts.

The electron-beam microprobe analysis of experiments A, B, E, and F was completed. Partly as a result of the swelling of the fuel pellets, mentioned above, there was much contact lost between the fuel pellet and the respective ceramic inserts. In the two experiments A and F there were regions of solid-solid contact as seen in both the optical and electron microprobe work. In experiments B and E no contact was seen in the polished couples. This, however, does not mean that there could not have been solid-solid contact during the experiment. The separation of the inserts and fuel pellets could have occurred due to mounting or transporting the couple.

In experiment A the study of the solid-solid contact area showed that interdiffusion did occur. The data showed that curium had migrated into the ThO_2 to an extent of three mils. The thorium had migrated into the $^{244}\text{Cm}_2\text{O}_3$ to an extent of two mils.

No contact areas were observed in experiments B and E. The data collected showed that no interdiffusion had occurred.

There were contact areas in experiment F. The data showed that curium had not migrated into the ZrO_2 . However, the zirconium had migrated into the $^{244}\text{Cm}_2\text{O}_3$ to an extent of three mils. A study of areas where there was no solid-solid contact did not show any interdiffusion.

In both the $ZrO_2-^{244}Cm_2O_3$ compatibility couples (experiments E and F) there was a darker gray phase completely surrounding only the $^{244}Cm_2O_3$ pellet. This phase was approximately 1.5 mils in thickness. The phase was observed both optically and with the electron-beam microprobe. After studying the darker gray phase with the electron-beam microprobe, it was concluded that the area was rich in calcium. The concentration of curium in this area appeared to be the same as in the bulk of the Cm_2O_3 pellet. The source of the calcium is not identified at this time.

Experiments C, G, and I have undergone their prescribed heating times in vacuum. In these experiments, the couples were fueled with pellets which had been fabricated the same day, and the couples were taken to temperature immediately after fueling. This was done in order to minimize the helium accumulation in the pellets, thus reducing the possibility of pellet expansion and loss of contact area.

FY 1974 Compatibility Matrix (*J. R. DiStefano and C. L. Ottinger*)

Materials selection and test assembly designs for a 15-couple matrix to be initiated during FY 1974 have been finalized. This matrix will include representatives of several types of potential encapsulation materials. The test assemblies will contain materials specimens which will be used to test tensile strength changes. Conditions of the tests and materials are shown below.

5000 hr, 900°C Helium	5000 hr, 1100°C Vacuum	10,000 hr, 1400°C Vacuum
Haynes-188	Pt-3008	Iridium
Ta-10% W	Iridium	Ir-2% W
Mo-46% Re	Ir-2% W	Mo-46% Re
TZM	Ta-10% W	W-26% Re
ZrO ₂ ^a	Mo-46% Re	
Si ₃ N ^a		

^aNo tensile specimen.

Reaction of Cm_2O_3 With Pt-26% Rh-8% W Alloy (*E. E. Ketchen*)

The alloy Pt-26% Rh-8% W (53.33 atom % Pt, 39.82 atom % Rh, 6.86 atom % W) is being considered as a capsule material to contain $^{244}Cm_2O_3$ heat source material. The potential for the reaction of Cm_2O_3 source material with Pt-26% Rh-8% W over the 600-1300°C temperature range was investigated from a thermodynamic viewpoint.

The purification of the curium produced includes plutonium removal. However, the curium product probably would be held at least a year after the purification step before it is fabricated as a heat source. During this period of time about 5% of the ^{244}Cm would have decayed to ^{240}Pu . The procedure used to reduce the CmO_2 to Cm_2O_3 before the fabrication step

would not convert the PuO_2 to Pu_2O_3 . Hence the plutonium is present as PuO_2 in the Cm_2O_3 product. For purposes of this thermodynamic study, it was assumed that the Cm_2O_3 contained 5 mole % PuO_2 .

The thermodynamic data needed to calculate the free energy of mixing of 95 mole % Cm_2O_3 with 5 mole % PuO_2 are not available. Since this partial molar free energy of mixing is probably small, it was neglected in the following calculations.

The partial molar free energies of mixing of Pt, W, and Rh were calculated using the following equation.²

$$\Delta\bar{G}_k = RT \ln x_k + V_k \left[\sum_i (\delta_k - \delta_i) \phi_i \right]^2 \quad (1)$$

where

$\Delta\bar{G}_k$ = Gibbs partial molar free energy of the k'th component

R = 1.9872 cal

T = absolute temperature

x_k = mole fraction of the k'th component

V_k = volume of the k'th component

δ_k = solubility parameter of the k'th component

δ_i = solubility parameter of the i'th component

ϕ_i = volume fraction of the i'th component

The solubility parameters were taken from data by Hildebrand and Scott.² In the derivation of Eq. 1, it was assumed that there was no compound formation of the metals with each other. The partial molar free energies are shown in Table 4 at 600-1300°C.

Table 4. Partial Molar Free Energies of Mixing of Components in Pt-26% Rh-8% W

Temperature (°C)	$-\Delta\bar{G}$ (cal/mole)		
	Pt	W	Rh
600	979	4407	1563
800	1229	5471	1930
1000	1481	6535	2294
1200	1728	7602	2262
1300	1853	8134	2845

The free energies of formation of Pt_3O_4 , WO_2 , Rh_2O , Cm_2O_3 , PuO_2 , and Pu_2O_3 were calculated from a data compilation by Alvin Glassner³ and a review article by F. L. Oetting⁴ and are shown in Table 5. Since the free energies of Pt_3O_4 are positive, this reaction will not proceed in the presence of oxygen at 600–1300°C. However, the free energies of tungsten and rhodium with oxygen over the 600–1300°C temperature range are negative, and these reactions could proceed.

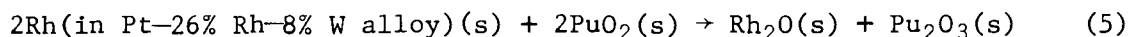
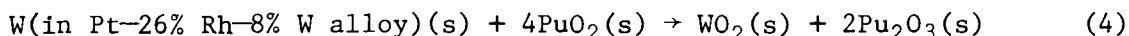
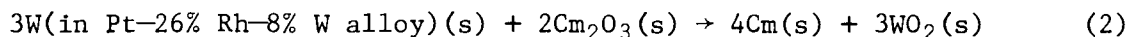
Table 5. Gibbs Free Energy of Formation of Pt_3O_4 , WO_2 , Rh_2O , PuO_2 , and Pu_2O_3

Temperature (°C)	ΔG_f (cal/mole)				
	Pt_3O_4	WO_2	Rh_2O	PuO_2	Pu_2O_3^a
600	10,300	-101,160	-11,350	-215,550	-352,120
800	26,400	-93,850	-9,090	-207,050	-339,320
1000	42,080	-86,780	-6,940	-198,700	-326,940
1200	57,330	-79,960	-4,900	-190,530	-314,980
1300	64,790	-76,800	-3,910	-186,500	-309,150

^a Pu_2O_3 data used as stand-in for Cm_2O_3 .

The free energy data for Pu_2O_3 were used as a stand-in for Cm_2O_3 over the 600–1300°C temperature range. At higher temperature, where the free energies of Cm_2O_3 could be calculated, the Pu_2O_3 values were in good agreement with Cm_2O_3 . Hence the use of the free energy values of Pu_2O_3 as a substitute for Cm_2O_3 may be a reasonable approximation.

The free energies from Tables 4 and 5 were used to calculate the free energy for Eqs. 2–5. The free energy for Eqs. 2–5 are shown in Table 6.



Since the free energies are positive for Eqs. 2–5, WO_2 and Rh_2O should not be formed at 600–1300°C. The above oxides are the most favorable oxides to be formed. Hence, the interaction between Cm_2O_3 and Pt–26% Rh–8% W to produce the oxides of platinum, rhodium, and tungsten would not be expected. It was assumed that there is no compound formation between the constituents of the alloy and that the curium metal will not form intermetallic compounds with constituents of the alloy. No oxygen solubility in the alloy is also assumed. Experimental verification of the results is needed.

Table 6. Gibbs Free Energies of Reaction for Eqs. 2-5

Temperature (°C)	ΔG_r (cal/mole of Cm_2O_3 or PuO_2)			
	Eq. 2	Eq. 3	Eq. 4	Eq. 5
600	206,990	327,450	15,300	35,380
800	206,750	323,630	15,290	34,770
1000	206,560	319,840	15,170	34,060
1200	206,450	316,260	14,950	33,250
1300	206,150	314,490	14,780	32,830

Reaction of Cm_2O_3 With T-111 Alloy (*E. E. Ketchen*)

The alloy T-111 (90.09 atom % Ta, 7.88 atom % W, and 2.03 atom % Hf) is being considered as a capsule material to contain $^{244}\text{Cm}_2\text{O}_3$ heat source material. The potential for the reaction of Cm_2O_3 source material with T-111 alloy over the 600-1300°C temperature range was investigated from a thermodynamic viewpoint.

The partial molar free energies of mixing for Ta, W, and Hf were calculated using the method described in the previous section, "Reaction of Cm_2O_3 With Pt-26% Rh-8% W Alloy." The results are shown in Table 7 from 600-1300°C. It should be noted again that this method of calculation assumes no compound formation of the metals with each other.

Table 7. Partial Molar Free Energies of Mixing of Components in T-111

Temperature (°C)	$-\Delta\bar{G}$ (cal/mole)		
	Ta	W	Hf
600	170	4347	6,604
800	222	5358	8,154
1000	264	6368	9,707
1200	293	7378	11,255
1300	326	7883	12,030

The free energies of formation of Ta_2O_5 , WO_2 , HfO_2 , Cm_2O_3 , PuO_2 , and Pu_2O_3 were calculated from a data compilation by Glassner³ and a review article by Oetting.⁴ The results are shown in Table 8. Since the free energies of formation of Ta_2O_5 , WO_2 , and HfO_2 are negative over the 600-1300°C temperature range, the metals will react with oxygen.

Table 8. Gibbs Free Energy of Formation
of Ta₂O₅, WO₂, HfO₂, PuO₂, and Pu₂O₃

Temperature (°C)	-ΔG _f (cal/mole)				
	Ta ₂ O ₅	WO ₂	HfO ₂	PuO ₂	Pu ₂ O ₃ ^a
600	395,690	101,160	225,450	215,550	352,120
800	374,820	93,850	216,450	207,050	339,320
1000	354,180	86,780	207,770	198,700	326,940
1200	333,750	79,960	199,260	190,530	314,980
1300	323,630	76,800	195,040	186,500	309,150

^aPu₂O₃ data used as stand-in for Cm₂O₃.

The free energies from Tables 7 and 8 were used to calculate the free energy for Eqs. 6-11. Results are shown in Table 9.

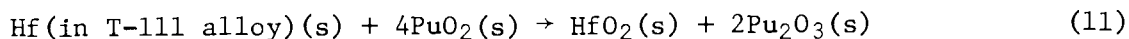
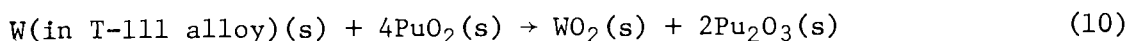
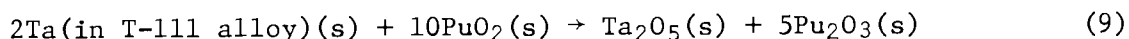
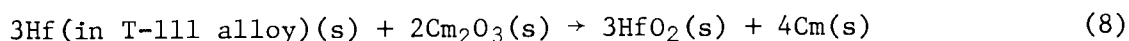
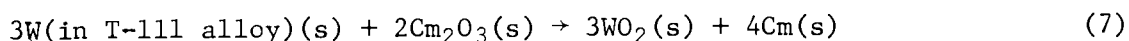
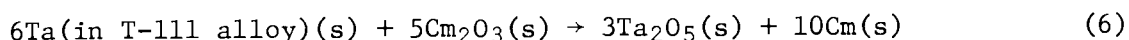


Table 9. Gibbs Free Energies of Reaction for Eqs. 6-11

Temperature (°C)	ΔG _r (cal/mole of Cm ₂ O ₃ or PuO ₂)					
	Eq. 6	Eq. 7	Eq. 8	Eq. 9	Eq. 10	Eq. 11
600	114,910	206,900	23,850	-48	15,280	-15,230
800	114,690	206,590	26,880	-53	15,260	-14,690
1000	114,750	206,330	29,840	-130	15,130	-15,280
1200	115,080	206,110	33,000	-280	14,900	-13,960
1300	115,360	205,780	34,610	-360	14,710	-13,810

Since the free energies for Eqs. 6-8 are positive, the T-111 alloy is not expected to react with pure Cm₂O₃. However, since the curium product will contain PuO₂, probably about 5%, the reaction of PuO₂ with T-111 was considered. Since the free energies for Eqs. 9 and 11 are negative, the PuO₂ in the curium product would be expected to react with the tantalum and hafnium in the T-111 alloy. It was assumed that there is no compound

formation between the constituents of the alloy or with the curium metal. No oxygen solubility in the alloy is also assumed.

In conclusion, it may be stated that a reaction between the tantalum and hafnium of the T-111 alloy and the PuO_2 would be expected. Experimental verification of the calculations is needed.

Reaction of Cm_2O_3 With Hafnalloy 20-20 (*E. E. Ketchen*)

The Hafnalloy 20-20 (95.78 atom % Hf, 3.71 atom % Sn, 0.33 atom % Pd, and 0.18 atom % Pt) is one of the materials under consideration as a capsule material to contain $^{244}\text{Cm}_2\text{O}_3$ heat source. The potential for the reaction of Cm_2O_3 source material with Hafnalloy 20-20 over the 600-1300°C temperature range was investigated from a thermodynamic viewpoint.

The partial molar free energies of mixing for Hf, Sn, Pd, and Pt were calculated using the method reported in the Section, "Reaction of Cm_2O_3 With Pt-26% Rh-8% W Alloy." The results are shown in Table 10 from 600-1300°C. The method of calculation of the partial molar free energies assumes that no compound formation is present in the alloy mixture.

Table 10. Partial Molar Free Energies of Mixing of Components in Hafnalloy 20-20

Temperature (°C)	$-\Delta\bar{G}$ (cal/mole)			
	Hf	Sn	Pd	Pt
600	18	4495	9,997	11,109
800	35	5816	12,118	13,331
1000	52	7110	14,542	16,109
1200	69	8425	16,725	18,499
1300	78	9080	17,861	19,756

The free energies of formation of HfO_2 , SnO_2 , PdO , Pt_3O_4 , Cm_2O_3 , PuO_2 , and Pu_2O_3 were calculated from a data compilation by Glassner³ and a review article by Oetting.⁴ The results are shown in Table 11. Since the free energies of formation of HfO_2 and SnO_2 are negative, they should react with oxygen over the 600-1300°C temperature range.

Table 11. Gibbs Free Energies of Formation of HfO₂, SnO₂, PdO, Pt₃O₄, PuO₂, and Pu₂O₃

Temperature (°C)	ΔG_f (cal/mole)					
	HfO ₂	SnO ₂	PdO	Pt ₃ O ₄	PuO ₂	Pu ₂ O ₃ ^a
600	-225,450	-95,730	-52	10,300	-215,550	-352,120
800	-216,450	-85,830	4,520	26,400	-207,090	-339,320
1000	-207,770	-76,080	8,780	42,080	-198,700	-326,940
1200	-199,260	-66,470	12,770	57,330	-190,530	-314,980
1300	-195,040	-61,710	14,620	64,790	-186,500	-309,150

^aPu₂O₃ data used as stand-in for Cm₂O₃.

The free energies from Tables 10 and 11 were used to calculate the free energies for Eqs. 12-17. Results are shown in Table 12.

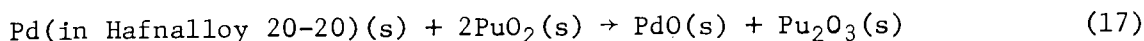
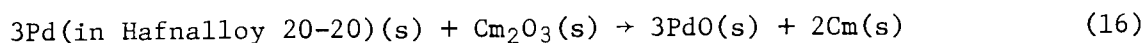
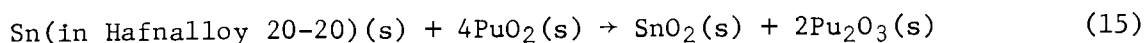
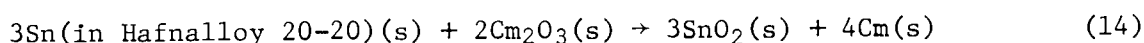
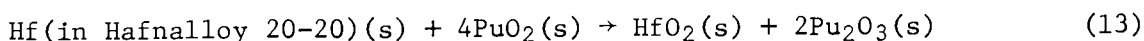
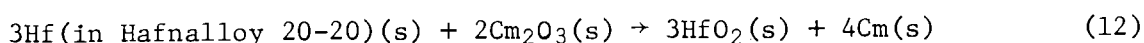


Table 12. Gibbs Free Energies of Reaction for Eqs. 12-17

Temperature (°C)	ΔG_r (cal/mole of Cm ₂ O ₃ or PuO ₂)					
	Eq. 12	Eq. 13	Eq. 14	Eq. 15	Eq. 16	Eq. 17
600	13,970	-16,870	215,270	16,680	382,000	44,460
800	14,700	-16,720	219,300	17,380	389,230	45,710
1000	15,320	-16,700	223,450	17,990	396,870	46,900
1200	16,200	-16,760	227,920	18,520	403,460	47,510
1300	16,700	-16,800	230,200	18,790	406,610	48,190

Only the hafnium of the alloy has a negative free energy of reaction (Eq. 13) with PuO₂. Hence, the reaction of hafnium with the PuO₂ is the only expected reaction of those considered. It was assumed that there is no compound formation between the constituents of the alloy or with the curium metal. No oxygen solubility in the alloy is assumed. Experimental verification of the results is needed.

Reaction of Cm_2O_3 With Stainless Steel 316 Alloy (*E. E. Ketchen*)

Stainless steel 316 alloy (65.08 atom % Fe, 18.14 atom % Cr, 11.34 atom % Ni, 2.02 atom % Mn, 1.97 atom % Si, and 1.45 atom % Mo) is one of the materials under consideration as a capsule material to contain $^{244}\text{Cm}_2\text{O}_3$ heat sources. The potential for the reaction of Cm_2O_3 source material with stainless steel 316 over the 600–1300°C temperature range was investigated from a thermodynamic viewpoint.

The partial molar free energies of mixing of Fe, Cr, Ni, Mn, Si, and Mo to give stainless steel 316 were calculated using the method reported in the Section, "Reaction of Cm_2O_3 With Pt–26% Rh–8% W Alloy." The results from 600–1300°C are shown in Table 13. This method of calculation of the partial molar free energies assumes that no compound formation is present in the alloy. It also assumes no oxygen solubility in the alloy.

Table 13. Partial Molar Free Energies of Mixing of Elements in Stainless Steel 316

Temperature (°C)	$-\bar{\Delta G}$ (cal/mole)					
	Fe	Cr	Ni	Mn	Si	Mo
600	730	2,900	3,640	6,710	6,650	7,320
800	900	3,580	4,490	8,260	8,210	9,010
1000	1,070	4,260	5,330	9,810	9,770	10,690
1200	1,240	4,930	6,180	11,360	11,800	12,370
1300	1,320	5,270	6,610	12,140	12,110	13,210

The free energies of formation of Fe_3O_4 , Cr_2O_3 , NiO, MnO, SiO_2 , MoO_2 , PuO_2 , and Pu_2O_3 were calculated from a data compilation by Glassner³ and a review article by Oetting.⁴ The results are shown in Table 14. The free energies of formation of Cm_2O_3 are assumed to be the same as the free energies of formation of Pu_2O_3 .

Table 14. Gibbs Free Energies of Formation of Fe_3O_4 , Cr_2O_3 , NiO, MnO, SiO_2 , MoO_2 , PuO_2 , and Pu_2O_3

Temperature (°C)	$-\Delta G_f$ (kcal/mole)							
	Fe_3O_4	Cr_2O_3	NiO	MnO	SiO_2	MoO_2	PuO_2	Pu_2O_3^a
600	199.79	203.92	39.06	76.82	172.92	95.60	215.55	352.12
800	185.20	189.81	35.01	73.30	164.60	87.91	207.05	339.32
1000	170.88	175.72	31.01	69.76	156.33	80.36	198.70	326.94
1200	156.61	161.67	27.10	66.23	148.10	72.94	190.53	314.98
1300	149.47	154.63	25.15	64.27	144.00	69.27	186.50	309.15

^a Pu_2O_3 data are used as a stand-in for Cm_2O_3 .

The free energies from Tables 13 and 14 were used to calculate the free energies for Eqs. 18-29. Results are shown in Tables 15 and 16.

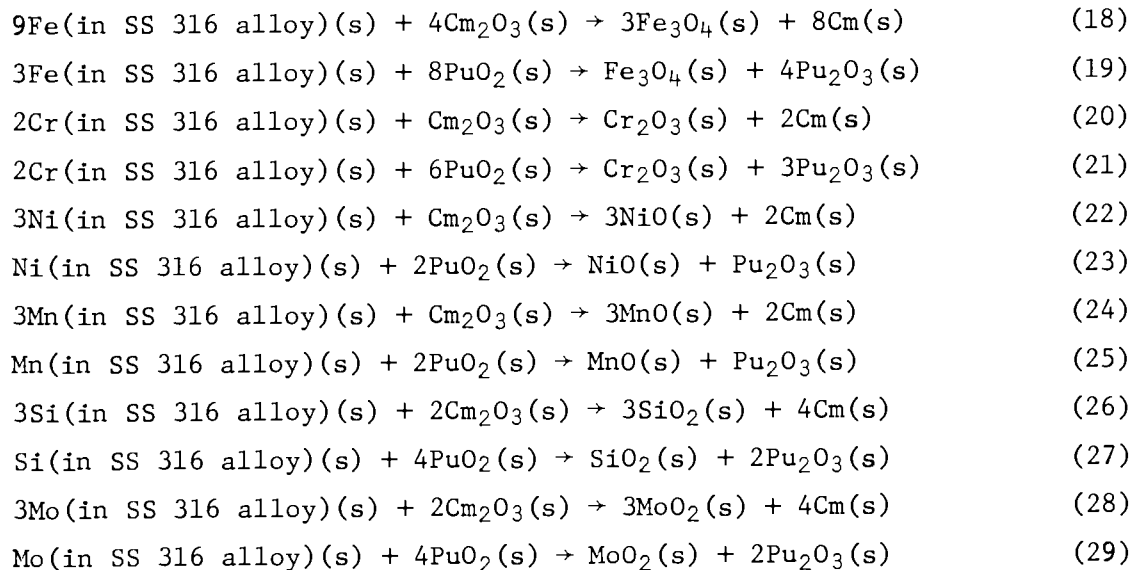


Table 15. Gibbs Free Energies of Reaction
for Eqs. 18, 20, 22, 24, 26, and 28

Temperature (°C)	ΔG_r (cal/mole of Cm_2O_3)					
	Eq. 18	Eq. 20	Eq. 22	Eq. 24	Eq. 26	Eq. 28
600	203,920	154,000	245,850	141,790	102,710	219,710
800	202,450	156,660	247,750	144,200	104,740	220,970
1000	201,150	159,690	249,870	147,060	107,060	222,400
1200	200,300	163,180	252,240	150,380	110,540	224,130
1300	200,020	165,060	253,520	152,770	111,310	225,060

Since the only negative free energies of reaction for Eqs. 18-29 are the reactions of PuO_2 with silicon, the silicon of stainless steel 316 is the only component that is expected to interact with the PuO_2 of the curium product in the 600-1300°C temperature range. It was assumed that there was no compound formation between the constituents of the alloy or with the curium metal. No oxygen solubility in the alloy was assumed. Experimental verification of the interaction of the silicon of stainless steel 316 is needed.

Table 16. Gibbs Free Energies of Reaction
for Eqs. 19, 21, 23, 25, 27, and 29

Temperature (°C)	ΔG_r (cal/mole of PuO_2)					
	Eq. 19	Eq. 21	Eq. 23	Eq. 25	Eq. 27	Eq. 29
600	14,790	6,470	21,770	4,430	-2,080	17,670
800	14,570	6,940	22,120	4,870	-1,710	17,660
1000	14,280	7,370	22,400	5,260	-1,410	17,820
1200	13,930	7,740	22,580	5,610	-1,040	17,900
1300	13,740	7,910	22,660	5,860	-1,030	17,930

Reaction of Cm_2O_3 With Ir-2% W Alloy (*E. E. Ketchen*)

The alloy Ir-2% W (97.91 atom % Ir, 2.09 atom % W) is one of the alloys being considered as a capsule material to contain the $^{244}\text{Cm}_2\text{O}_3$ heat source material.

The partial molar free energies of mixing for iridium and tungsten were calculated using the method reported in the Section, "Reaction of Cm_2O_3 With Pt-26% Rh-8% W Alloy." The results are shown in Table 17. It should be noted that these calculations assume that there is no compound formation between the iridium and tungsten.

Table 17. Partial Molar Free Energies
of Mixing of Components of Ir-2% W Alloy

Temperature (°C)	$-\Delta\bar{G}$ (cal/mole)	
	Iridium	Tungsten
600	37	6,710
800	45	7,900
1000	53	9,780
1200	62	11,320
1300	66	12,090

The free energies of formation of Ir_2O_3 , WO_2 , Pu_2O_3 , and PuO_2 were calculated from a data compilation by Glassner³ and a review article by Oetting.⁴ The results are shown in Table 18. Iridium will react with oxygen at 600 and 800°C, and tungsten will react with oxygen at 600-1300°C.

Table 18. Gibbs Free Energies of Formation of Ir₂O₃, WO₂, Pu₂O₃, and PuO₂

Temperature (°C)	-ΔG _f (kcal/mole)			
	Ir ₂ O ₃	WO ₂	Pu ₂ O ₃ ^a	PuO ₂
600	-13,900	-101,160	-352,120	-215,550
800	-2,450	-93,850	-339,320	-207,050
1000	8,610	-86,780	-326,940	-198,700
1200	19,490	-79,960	-314,980	-190,530
1300	24,040	-76,800	-309,150	-186,500

^aPu₂O₃ data are used as a stand-in for Cm₂O₃.

The free energies from Tables 17 and 18 were used to calculate the free energies for Eqs. 30-33. Results are shown in Table 19.

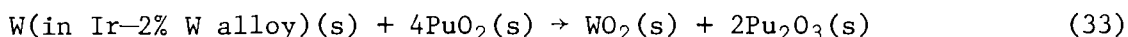
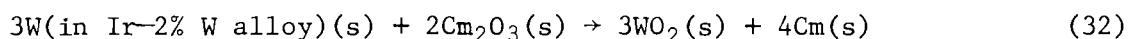
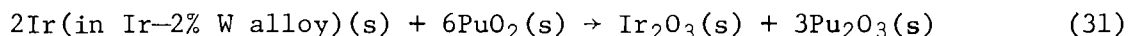
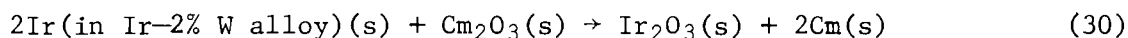


Table 19. Gibbs Free Energies of Reaction for Eqs. 30-33

Temperature (°C)	ΔG _r (cal/mole of Cm ₂ O ₃ or PuO ₂)			
	Eq. 30	Eq. 31	Eq. 32	Eq. 33
600	338,290	37,180	210,430	15,870
800	336,960	36,990	210,930	15,900
1000	335,650	36,690	211,450	15,990
1200	334,600	36,310	212,020	15,880
1300	333,320	35,960	212,080	15,750

Since the free energies are positive for the reaction to form Ir₂O₃ and WO₂ from the alloy and Cm₂O₃ and PuO₂, this reaction should not occur at 600-1300°C.

In conclusion, it appears from thermodynamic considerations that the Ir-2% W alloy will not react with the Cm₂O₃ fuel containing 5% PuO₂ at 600-1300°C. The calculations were made on the assumption that there is no compound formation between iridium and tungsten or curium metal and the alloy. The oxides most likely to be produced were considered. No assumptions were made as to the solubility of oxygen in the alloy. Experimental verification of the calculations is needed.

Reaction of Cm_2O_3 With Pt-30% Rh-8% W (*E. E. Ketchen*)

The alloy Pt-30% Rh-8% W (48.68 atom % Pt, 44.65 atom % Rh, and 6.66 atom % W) is one of the alloys being considered as a capsule material to contain the $^{244}\text{Cm}_2\text{O}_3$ heat source material.

The partial molar free energy of mixing for platinum, rhodium, and tungsten were calculated using the method described in the Section, "Reaction of Cm_2O_3 With Pt-26% Rh-8% W Alloy." The results are shown in Table 20. It should be noted that these calculations assume that there is no compound formation between platinum, rhodium, and tungsten.

Table 20. Partial Molar Free Energies of Mixing of Components of Pt-30% Rh-8% W

Temperature (°C)	$-\Delta\bar{G}$ (cal/mole)		
	Pt	Rh	W
600	1130	1370	4470
800	1420	1690	5550
1000	1710	2010	6630
1200	2090	2330	7700
1300	2130	2490	8240

The free energies of formation of Pt_3O_4 , Rh_2O , WO_2 , Pu_2O_3 , and PuO_2 were calculated from a data compilation by Glassner³ and a review article by Oetting.⁴ The results are shown in Table 21. Platinum will not react with oxygen at 600-1300°C, but rhodium and tungsten will react with oxygen at 600-1300°C.

Table 21. Gibbs Free Energy of Formation of Pt_3O_4 , Rh_2O , WO_2 , Pu_2O_3 , and PuO_2

Temperature (°C)	ΔG_f (kcal/mole)				
	Pt_3O_4	Rh_2O	WO_2	Pu_2O_3^a	PuO_2
600	10,300	-11,350	-101,160	-352,120	-215,550
800	26,400	-9,090	-93,850	-339,320	-207,050
1000	42,080	-6,940	-86,780	-326,940	-198,700
1200	57,330	-4,900	-79,960	-314,980	-190,530
1300	64,790	-3,910	-76,800	-309,150	-186,500

^a Pu_2O_3 data are used as a stand-in for Cm_2O_3 .

The free energies from Tables 20 and 21 were used to calculate the free energies for Eqs. 34-37. Results are shown in Table 22.

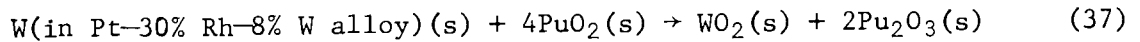
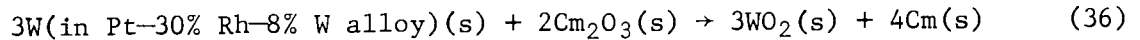
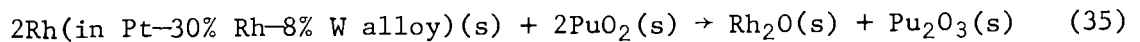
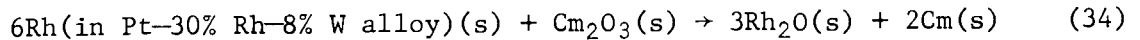


Table 22. Gibbs Free Energies of Reaction for Eqs. 34-37

Temperature (°C)	ΔG_r (cal/mole of Cm_2O_3 or PuO_2)			
	Eq. 34	Eq. 35	Eq. 36	Eq. 37
600	326,290	35,180	207,080	15,310
800	322,190	34,530	206,880	15,310
1000	318,170	33,770	206,710	15,190
1200	314,270	32,920	205,600	14,980
1300	312,360	32,480	206,320	14,800

Since the free energies are positive for the reaction to form Rh_2O and WO_2 from the alloy and Cm_2O_3 and PuO_2 , this reaction should not occur at 600-1300°C.

In conclusion, it appears from thermodynamic considerations that the Pt-30% Rh-8% W alloy will not react with the Cm_2O_3 fuel containing 5% PuO_2 at 600-1300°C. The calculations were made on the assumption that there is no compound formation between platinum, rhodium, and tungsten or curium metal and the alloy. The oxides most likely to be produced were considered. No assumptions were made as to the solubility of oxygen in the alloy. Experimental verification of the calculations is needed.

Reaction of Cm_2O_3 With Carbon (*E. E. Ketchen*)

The reaction of Cm_2O_3 with carbon is of interest in the $^{244}\text{Cm}_2\text{O}_3$ heat source program. The thermodynamic calculations⁵ on the reaction of Cm_2O_3 with carbon to produce CmO have been extended to include Cm , $\text{CmC}_{0.5}\text{O}_{0.5}$, $\text{CmC}_{0.9}$, $\text{CmC}_{1.5}$, and CmC_2 as reaction products.

The free energies were calculated from data by F. L. Oetting,⁴ *JANAF Thermochemical Tables*,⁶ and data by R. A. Kent.⁷ Plutonium data for Pu_2O_3 , Pu , $\text{PuC}_{0.5}\text{O}_{0.5}$, $\text{PuC}_{0.9}$, $\text{PuC}_{1.5}$, and PuC_2 were used as stand-ins for the curium compound data. The results are shown in Table 23 between 1700 and 2400°K. The free energies were calculated for the compound formation by the reaction of Cm_2O_3 and carbon at the temperatures for

which the data were derived. Since the free energies are all positive, no reaction is expected at the temperatures investigated unless a product of reaction such as CO is removed. Curium dicarbide may be formed above 2300°K where the free energy may become negative.

Table 23. Gibbs Free Energies of Reaction of Cm_2O_3 With Carbon to Produce Cm, $\text{CmC}_{0.5}\text{O}_{0.5}$, $\text{CmC}_{0.9}$, $\text{CmC}_{1.5}$, and CmC_2

Temperature (°K)	ΔG_r (kcal/mole of compound)				
	Cm	$\text{CmC}_{0.5}\text{O}_{0.5}$	$\text{CmC}_{0.9}$	$\text{CmC}_{1.5}$	CmC_2
1700	57.45	41.57	47.25	47.10	
1800	51.61	38.94	41.45	41.47	
1900	45.83			35.90	
2000	40.10				21.36
2100	34.40				15.11
2200	28.76				8.91
2300	23.20				2.79
2400	18.73				

A thermodynamic investigation⁷ has been made on the reaction of PuO_2 and carbon to form Pu, $\text{PuC}_{0.5}\text{O}_{0.5}$, $\text{PuC}_{0.9}$, $\text{PuC}_{1.5}$, and PuC_2 . Table 24 shows the results of this work. Unless the products of reaction are removed there should be no carbide formation until the temperature is near 2150°K.

Table 24. Gibbs Free Energies of Reaction of Carbon With PuO_2 to Produce Pu, $\text{PuC}_{0.5}\text{O}_{0.5}$, $\text{PuC}_{0.9}$, $\text{PuC}_{1.5}$, and PuC_2

Temperature (°K)	ΔG_r (kcal/mole of compound)				
	Pu	$\text{PuC}_{0.5}\text{O}_{0.5}$	$\text{PuC}_{0.9}$	$\text{PuC}_{1.5}$	PuC_2
1700	56.37	41.6	43.6	38.5	
1800	48.32	35.6	35.5	30.2	
1900	40.28			22.0	
2000	33.17				13.5
2100	24.15				4.9
2200	16.18				-3.7
2300	8.20				-12.2

$^{244}\text{Cm}_2\text{O}_3$ Property CharacterizationHelium Release (*P. Angelini*)

The final vacuum checks have been completed on the furnaces and headers. The three molybdenum sample tubes have been outgassed to 1900°C.

A paper containing the results of previous experiments on helium release from $^{244}\text{Cm}_2\text{O}_3$ has been sent to the publisher.

Vapor Pressure (*P. Angelini and J. C. Posey*)

The temperature capability of the high-temperature vacuum furnace was tested. The unit is capable of achieving temperatures of at least 1900°C.

Part of the vacuum system associated with this furnace has been modified. The liquid nitrogen cold trap has been received and installed in the vacuum system. Some leaks were found in the main vacuum line and roughing valve by using a helium leak detector. The leaks were repaired and the unit reinstalled and checked. The system is now operating satisfactorily and is able to achieve pressures less than 5×10^{-6} torr at furnace temperatures up to 1900°C.

The mechanical chopper has been installed on the mass spectrometer furnace. A vacuum of $<5 \times 10^{-6}$ torr can be achieved with the motor installed and furnace temperatures up to 1600°C. However, the pressure goes up rapidly at higher furnace temperatures. If the outgassing problem cannot be solved, the mechanical chopper will not be included in the furnace.

X-Ray Diffraction (*P. Angelini*)

The written procedure and description of the x-ray diffraction glove box system were sent to the Safety Committee. The system has been approved for radioactive operation. The final alignment was performed with the furnace hot stage in place. Silicon powder specimens were used in this procedure. The equipment and supplies needed for the first planned experiment were gathered and placed in the process glove box.

The pellet used in the distilled water solubility test was transferred to the process glove box servicing the x-ray diffraction unit. The powder was taken from the water-filled transfer storage bottle, crushed, and left in air to dry before a sample was mounted on the lucite sample holder. After 24 hr the sample was mounted in the instrument and a scan made from 20 to 70 degrees (2θ). Both a monoclinic and an f.c.c. pattern were recorded. The f.c.c. pattern was more pronounced than the monoclinic pattern; however, the peaks were rather broad, showing some crystal damage. The lattice parameter calculated from the f.c.c. pattern was 5.384 Å. This can be compared with the annealed lattice parameter for PuO_2 and CmO_2 which have values of 5.386 Å and 5.372 Å, respectively. The powder from which the pellet was made contained 13% ^{240}Pu .

Three reasons could account for the large lattice parameter from the sample: the sample could be a hydrated oxide, it could be damaged by alpha radiation, or it could be largely PuO_2 . Thus a second sample was taken to 250°C in air for 2 hr. A scan was performed in air immediately after cooling. The f.c.c. pattern shifted. The monoclinic pattern decreased in strength relative to the f.c.c. The f.c.c. pattern resulted in a calculated lattice parameter of 5.369 Å. Thus it seems that this sample was mainly $^{244}\text{CmO}_2$. The initial sample was probably a hydrated form of the dioxide having a small fraction of unreacted Cm_2O_3 .

The second solubility pellet from the first seawater test was transferred to the process glove box in its water-filled storage container. The pellet was removed, crushed, and loaded onto the sample holder under an inert argon atmosphere. The pellet pieces could be broken very easily; however, it was not powderlike as in the first sample. The sample was loaded in the instrument and a scan performed from 10 to 82 degrees (2θ) under a helium purge. Again two patterns were observed. The f.c.c. pattern was again more intense than the monoclinic pattern; however, the difference was not as pronounced as in the other sample. The lattice parameter for the f.c.c. pattern was calculated to be 5.369 Å.

In this case, the value for the lattice parameter is very close to that of CmO_2 . The sample had been mounted on the holder in a wet condition. It is possible that, due to self heating and the sample being contained in a dry helium purge gas situation, the original powder could have dehydrated. More experimentation is needed to identify the exact nature of the compound soon after a solubility experiment is terminated.

The entry glove box to the process glove box was fabricated and installed. All safety requirements have been met and the unit was placed in operation. The complete safety interlock system is now installed. Some service to the ratemeter and power supply units has been performed. The graphite crystal has been received and bagged into the glove box. The crystal and the monochromator system is being installed onto the unit.

Emissivity (*P. Angelini*)

The testing of the spectroradiometer has begun. Minor vacuum leaks in the system have been located and are being removed. Shop work has had to be performed on some of the pieces. The spectroradiometer was tested to a maximum sample temperature of 1300°C . Various changes to the spectroradiometer have been made. A new furnace heat-shield system was designed. This should enable the attainment of higher sample temperatures.

Heat Capacity (*P. Angelini*)

The experimental equipment is ready for operation upon receipt of a pellet prepared from $^{244}\text{Cm}_2\text{O}_3$ freshly separated from $^{240}\text{PuO}_2$.

Dimensional Stability (*T. A. Butler and C. L. Ottinger*)

Two pellets of high-purity $^{244}\text{Cm}_2\text{O}_3$ were fabricated under identical pressing conditions. Furnace cycles, pressure increase patterns, and other conditions were controlled as closely as possible; the final pressing conditions were 4000 psi, 1450°C, and 30-min full pressure. Pellet data are shown below:

	<u>PCM-P1</u>	<u>PCM-P2</u>
Diameter (cm)	1.270	1.270
Height (cm)	0.795	0.794
Weight (g)	10.82	10.93
Density (g/cm ³)	10.8	10.9
Watts	25.8	26.0
Power density (W/cm ³)	25.6	25.8

Both pellets were excellent in appearance, showing no evidence of cracks or chips. Each pellet was stored on a platinum tray, with the pellet lying on its side to minimize conductive cooling and provide maximum surface exposure to atmosphere. Visual observation in the lighted cell (in argon atmosphere ~30°C) showed a barely detectable red glow around the midpoint of the cylindrical axis. However, with the cell lights out definite heat zones could be distinguished. The areas of highest intensity were the centers of the flat end faces and at the midpoint of the cylindrical axis. The color intensity decreased toward the edges (i.e., the periferies of the ends of the cylinder), and there was a zone of black, cooler material in the shape of a ring on either end. Although no actual temperature measurements were made, calculations using various assumptions gave average surface temperature values ranging from 640 to 690°C; this is in general agreement with the visual observation. The corresponding calculated maximum internal temperature range was 700 to 750°C.

Pellet PCM-P1 was exposed to dry air and pellet PCM-P2 was stored in argon. Periodic inspections were made including weighing and measurement of heights and diameters. During an inspection of PCM-P1 after 70 hr storage in air, it was noted that a small chip had broken off one edge. After 100 hr, both edges of PCM-P1 were chipped badly all around. The chipping did not occur during handling; pieces simply fell off the pellet. After ~10% of the pellet material had flaked off, no additional flaking occurred. Measurements of height and diameter (made across the unchipped sections) showed no changes. The measuring device could detect changes with a precision of 0.005 cm. Pellet PCM-P2 showed no changes in weight, height, or diameter during two weeks' storage in argon.

It is thought that the flaking of the air-exposed pellet resulted from oxidation of the Cm_2O_3 in the relatively cool zones at the pellet edges. This oxidation process can occur in the temperature range from 250 to 520°C. Although the average surface temperature is above this range, the cooler edge area temperature is probably within it. Stresses resulting from thermal gradients may be involved but are probably not the basic cause, as evidenced by the stability of the argon-stored pellet.

The relatively high density of these two pellets (~95% of theoretical) is interesting when compared to similar pellets made from production-grade material. A pellet of batch SR-31 was pressed under the identical procedure used for PCM-P1 and PCM-P2. The SR-31 pellet density was only 10.1 g/cm³ (weight, 10.88 g; height, 0.852 cm; diameter, 1.27 cm). Some indications of a relationship between fuel age and achievable density have been noted in the past, but there have been too few pellets fabricated to establish this relationship. Table 25 shows the average density of a few pellets with diameters 1.3 ± 0.1 cm pressed under similar conditions from fuels of different ages.

Table 25. Average ²⁴⁴Cm₂O₃ Pellet Densities

Identification	No. of Pellets	PuO ₂ Content (weight %) ^a	Average Density (g/cm ³)
PCM	2	<0.5	10.8
Kilowatt test	14	3.0	10.2
SR-31 test	1	8.5	10.1
Neutron source test	2	12.5	9.8

^aApproximate, at time of fabrication.

The age is expressed as PuO₂ content since this is the main age-dependent variable. Other factors may be involved, if indeed the effect is real, such as storage conditions and method of purification.

Rate of Dissolution of Cm₂O₃ in Seawater (*J. C. Posey*)

Measurements of the rate of loss of curium from the surface of hot-pressed ²⁴⁴Cm₂O₃ pellets in seawater have been carried out under two different sets of conditions. First the rate of loss to a stream of fresh air-saturated seawater at room temperature was measured. Next, the loss to a fixed volume of boiling seawater was determined.

The measurements in flowing seawater were carried out in the same manner as the previous measurements in flowing distilled water. This procedure was described in more detail last quarter.⁵

Samples of the stream of seawater that had passed over the pellet were taken at intervals and analyzed for curium content. Part of the samples were filtered using a 0.1- μ m filter to remove particulate matter. The dissolution rates were calculated from the curium contents of the samples, the seawater flow rate, and the area of the pellet.

After 1276 hr the pellet was removed from the flowing water system and independent measurements were made of the rate of loss of curium from its surface. The pellet was placed in a sample bottle containing seawater.

After 171 hr the pellet was removed from the seawater and placed in a second bottle of seawater. The total ^{244}Cm remaining in the first bottle was then determined. A sample of the water in the second bottle was taken after 42 hr. The total exposure time of the pellet to seawater was 1489 hr.

The measurement of the loss of curium by a pellet in boiling seawater was carried out in the following manner. The pellet was suspended in a platinum gauze basket in a Pyrex glass flask containing 175 ml seawater. Samples of water were withdrawn in pairs from the flask from time to time and analyzed for ^{244}Cm . One sample was withdrawn through a fine sintered glass filter; the other sample was not filtered. The test was continued for 847 hr.

At the end of the test the pellet was removed, nitric acid was added to the flask, and the solution was boiled for 24 hr to bring particulate material into solution. The pellets had a comparatively high plutonium content, 13.1% expressed as PuO_2 . Their densities were comparatively low, 8.5 and 6.8 g/cm^3 , respectively for the flowing water and boiling water tests.

No visible disintegration of the pellet occurred in either test using seawater. This behavior contrasts with that of Cm_2O_3 pellets in distilled water. Visible breakup of the pellet began after 300-400 hr in the flowing air-saturated distilled water at room temperature. In boiling distilled water, breakup was observed after only 8.4 hr.

The pellet exposed to seawater at room temperature, however, was found to be mechanically weak. It was easily crushed to a powder. Freshly hot-pressed Cm_2O_3 pellets are very hard and are very difficult to grind to a powder, indicating that a change in the pellet had occurred. X-ray diffraction indicated the presence of both Cm_2O_3 and CmO_2 . This work is described in more detail under "X-Ray Diffraction" above. The pellet exposed to boiling seawater has been preserved for other possible methods of examination.

The rate data obtained with flowing seawater are shown in Fig. 3. The first rate, 647 $\mu\text{g/cm}^2\cdot\text{hr}$ at 0.12 hr, was much higher than the subsequent rates and is not shown on Fig. 3. It indicates loose particulate material on the surface of the pellets. The same phenomenon was observed in the test using air-saturated distilled water.

The rates calculated from the concentrations of filtered samples average lower than those calculated from the concentrations of samples that were not filtered. This indicates the presence of particulate material and suggests that material leaves the surface by a mechanism other than simple solution.

After 300-400 hr a large increase was observed in the rates that were based on unfiltered samples. A similar increase was observed in the test using air-saturated distilled water at approximately the same time from the beginning of the test. In the distilled water test, however, a breaking up of the pellet was observed at the same time.

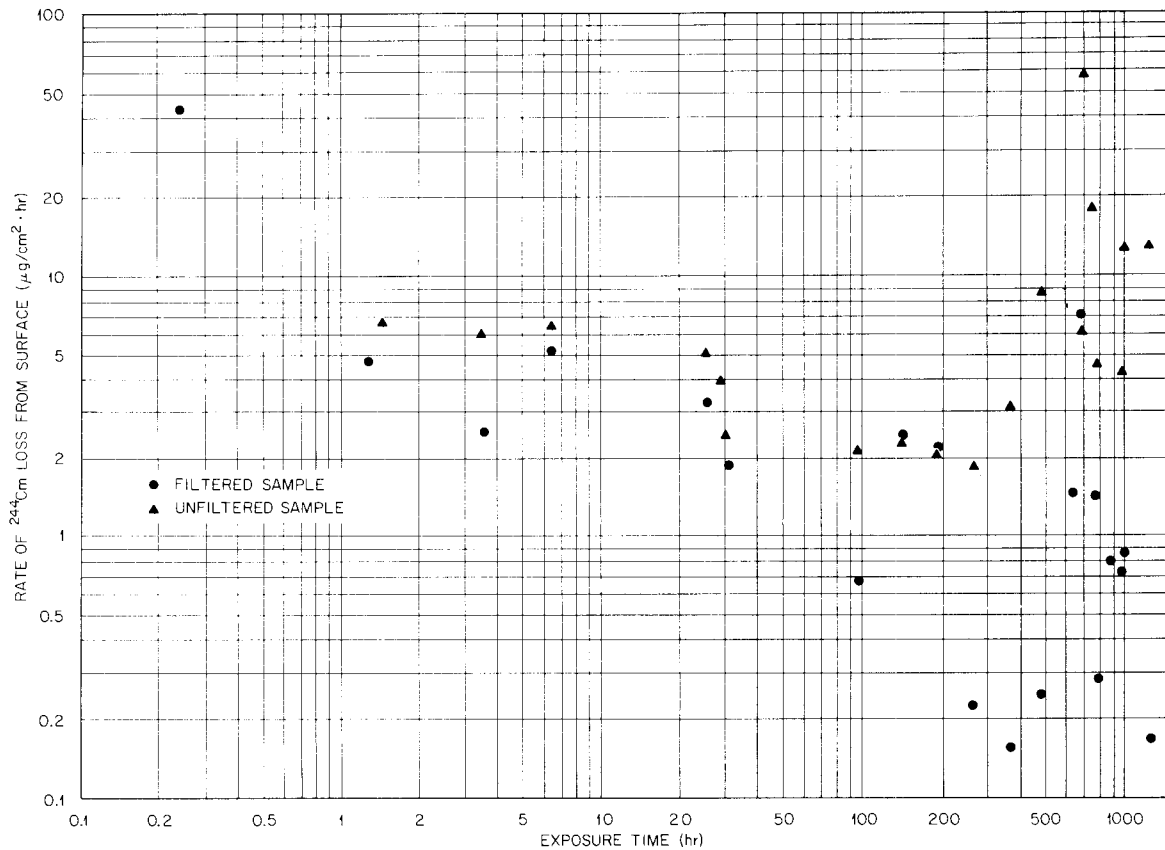


Fig. 3. Rate of Loss of ^{244}Cm From Surface of Pellet in Seawater.

The average rate of ^{244}Cm loss was $4 \mu\text{g}/\text{cm}^2 \cdot \text{hr}$ during the first 364 hr. This value is based on the samples which were not filtered excluding the first abnormally high value. The high values obtained after 364 hr were not used because of the probability that a chemical change in the pellet had occurred. Furthermore, gelatinous corrosion products appeared in the system at about this time. This added an element of uncertainty to the later data.

The two independent rate measurements carried out after the flowing water measurements gave values of $146.1 \mu\text{g}/\text{cm}^2 \cdot \text{hr}$ and $49 \mu\text{g}/\text{cm}^2 \cdot \text{hr}$, respectively, for the first and second tests. These values are compatible with the high values observed late in the flowing water test.

The results of the boiling water test are given in Table 26. The filtered samples had lower concentrations than the samples that were not filtered. This indicated the presence of particulate material. Both the filtered and unfiltered sample concentrations increased with time. The filtered sample concentrations probably do not represent material in true solution. The presence of suspended material throughout the test indicates that the solution was saturated. Colloidal material could have passed through the filters used.

Table 26. Dissolution of Cm_2O_3 in Boiling Seawater

Time (hr)	^{244}Cm Concentration in Seawater ($\mu\text{g}/\text{ml}$)	Average Rate of Dissolution From Beginning of Test ($\mu\text{g}/\text{cm}^2\cdot\text{hr}$)
3.6	0.0025 ^a	—
3.6	0.0082	0.64
29.2	0.0038 ^a	—
29.3	0.021	0.20
147.6	0.19 ^a	—
147.6	0.67	1.3
390.3	0.85 ^a	—
390.3	2.0	1.4
507	0.47 ^a	—
507	2.0	1.1
724	1.5 ^a	—
724	5.1	2.0
846	1.4 ^a	—
846	4.2	1.4
847	8.0 ^{a,b}	2.7
847	7.3 ^b	2.5

} 2.6 av

^aSample filtered.^bParticulate material brought into solution by acid.

The final concentrations, obtained after acid treatment, are appreciably higher than those obtained immediately before the acid addition. This indicates that some particulate material had settled out.

The overall average rate of dissolution was $2.6 \mu\text{g}/\text{cm}^2\cdot\text{hr}$. This value is lower than the value of $4 \mu\text{g}/\text{cm}^2\cdot\text{hr}$ obtained early in the test with flowing seawater at room temperature. It is much lower than the values obtained late in the room temperature test.

Reaction of Cm_2O_3 With Dry Air (*J. C. Posey*)

Measurements were made of the rate of gain in weight of a hot-pressed pellet exposed to dry air. The pellet was composed of Cm_2O_3 containing 13.1% $^{240}\text{PuO}_2$ decay product; the density was $7.4 \text{ g}/\text{cm}^3$ or 64% of theoretical. The pellet was exposed to air at room temperature; however, it was heated by radioactive decay. The estimated average surface temperature was 150°C .

The results are shown in Fig. 4. This low density material cannot be exposed to air without oxidation. Complete oxidation to CmO_2 , however, requires an extended period of time — in this case about 100 days.

Two samples of purified curium oxide were loaded into platinum cups in loose powder beds $\sim 1 \text{ cm}$ in diameter by 1.5 cm deep and calcined in vacuum 4 hr at 1000°C . Weight losses were 0.11 g and 0.12 g on samples containing 4.39 and 5.27 g of curium, respectively. Although not in exact

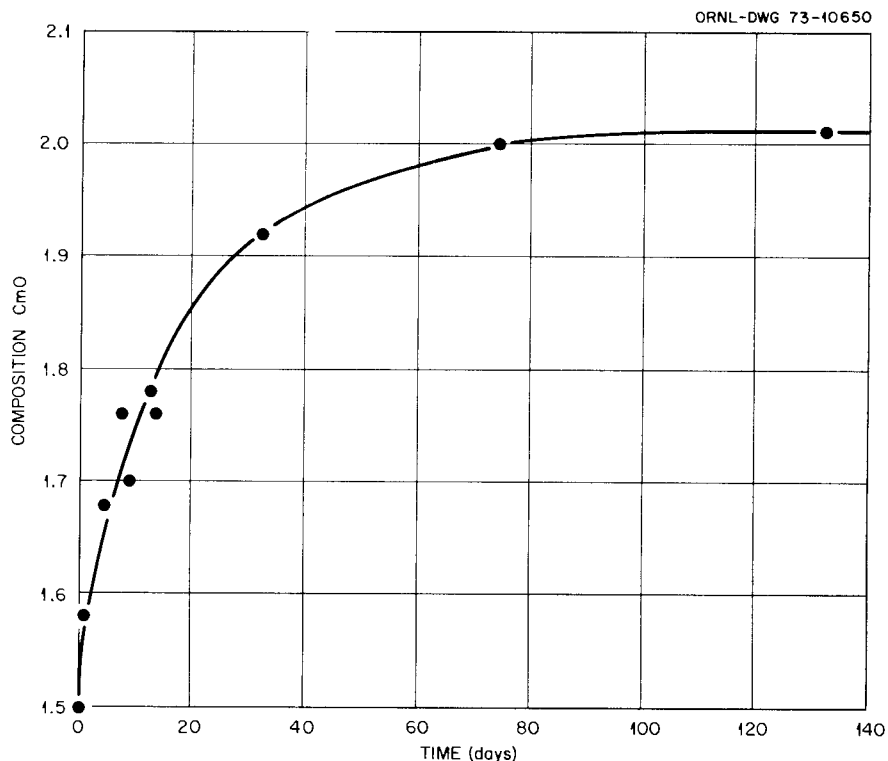


Fig. 4. Oxidation of Cm_2O_3 Exposed to Dry Air.

agreement, both samples indicate an original composition intermediate between $\text{CmO}_{1.8}$ and $\text{CmO}_{2.0}$. The two samples were exposed to dry air for 100 hr. Some weight gain was measured but neither sample returned to its original uncalcined weight. Another sample containing 9.94 g of curium was calcined under the same conditions but in a thin granular layer, then exposed to dry air and weighed periodically. The weight gain was ~ 0.07 g/day to a final stabilized weight which was 0.27 g above the calcined weight. The sample was again calcined and the weight loss was 0.26 g. These results also indicate an air-stabilized composition in the range of $\text{CmO}_{1.8}$ – $\text{CmO}_{2.0}$.

$^{244}\text{Cm}_2\text{O}_3$ Radiation Measurements (*K. W. Hauff*)

During some process equipment checks at the Curium Source Fabrication Facility, recalibration of the process calorimeter used to assay the $^{244}\text{Cm}_2\text{O}_3$ pellets in the source utilized in radiation spectra determinations resulted in an increase of $\sim 2\%$ in the calibration constant. The revised value for the source based on this recalibration was 68.8 W versus the original 67.3 W. Since the content of this source needed to be known accurately, a verification check was made using a different calorimeter which is large enough to accept the encapsulated source. First, the source was placed in the calorimeter and the EMF output of the thermopile was measured after a steady EMF output was obtained. Then

the source was replaced with an electric heater and the power adjusted until the EMF output was the same as that measured for the source. Since all conditions were the same for both runs, the possibilities for extraneous effects were minimized by this technique. The power input to the heater was measured at 68.5 W (69.1 W extrapolated to time of radiation measurements). This is a direct comparative value independent of calibration calculations and is considered the most accurate value for the source content.

The radiation measurements of the 69.1-W_t ²⁴⁴Cm₂O₃ source were completed, and the neutron data have been analyzed. The data for the neutron emission are presented in Table 27. A comparison of the new data with data previously reported by Savannah River⁸ in Table 28 shows that the total neutron emission per thermal watt is ~7.6% lower than the SRL data corrected for the 0.0576- to 0.3-MeV range not measured by SRL. This difference is probably within experimental error and is not considered significant.

Table 27. Neutron Spectra Data for ²⁴⁴Cm₂O₃
(Measured July-August 1973)

BIN (MeV)		Neutron Emission [$\phi(E)$, n/sec·W _t]
Low Edge	High Edge	
0.0576	0.0789	0.2878 × 10 ⁵
0.0789	0.1091	0.3196 × 10 ⁵
0.1091	0.1517	0.3807 × 10 ⁵
0.1517	0.2084	0.6631 × 10 ⁵
0.2084	0.2644	0.6044 × 10 ⁵
0.2644	0.3622	1.2921 × 10 ⁵
0.3622	0.5044	1.7558 × 10 ⁵
0.5044	0.7000	2.3975 × 10 ⁵
0.7000	1.0052	3.8578 × 10 ⁵
1.0052	1.400	4.5391 × 10 ⁵
1.0	1.5	5.7197 × 10 ⁵
1.5	2.	5.2860 × 10 ⁵
2.0	2.7	6.2799 × 10 ⁵
2.7	3	2.2421 × 10 ⁵
3	4	4.7010 × 10 ⁵
4	6	4.0072 × 10 ⁵
6	7	0.7389 × 10 ⁵
7	9	0.5177 × 10 ⁵
9	10.6	0.1242 × 10 ⁵
10.6	12	0.0348 × 10 ⁵

The ²⁴⁴Cm₂O₃ source was returned to the Tower Shielding Facility for rechecks on the low-energy neutron spectrum. The gamma data are presently being analyzed.

Table 28. Comparison of ORNL and SRL $^{244}\text{Cm}_2\text{O}_3$ Neutron Emissions Data

ORNL Data		SRL Data	
MeV Range	n/sec·W _t	MeV Range	n/sec·W _t
0.0576-1.0052	1.1559×10^6	0.0576-0.3 ^a	0.273×10^6
1.0-12.	2.9652×10^6	0.3-12.8 (S _f)	4.04×10^6
12.-12.8 ^b	0.0007×10^6	0.3-12.8 (α,n)	0.151×10^6
Total	4.1218×10^6		4.464×10^6

^aORNL data included for comparison.

^bSRL data included for comparison.

Impact Testing of Heat Source Materials (*D. W. Ramey*)

Since the impact testing of curium fuel has been postponed for a period of 1 year, provisions were made to store all equipment for the project. In addition to preparing various pieces of equipment for storage, a safety analysis was written for the operation of the impact gun in Room 12, Building 3026-C. This analysis will be subject to the review and approval of the ORNL Radiation Safety Review Committee.

Assay of SRL-31 Curium-244 Oxide (*T. A. Butler*)

Curium-244 oxide batch SRL-31 was assayed to provide additional $^{244}\text{Cm}_2\text{O}_3$ for characterization experiments. The isotopic abundances of the two principal elements, curium and plutonium, are given in Table 29.

Table 29. Isotopic Abundances of Curium and Plutonium in SRL-31 Oxide

Curium		Plutonium	
Mass No.	Isotopic Abundance (atom %)	Mass No.	Isotopic Abundance (atom %)
244	94.26	238	0.091
245	0.880	239	0.028
246	4.74	240	99.86
247	0.077	241	0.002
248	0.042	242	0.022
		244	$\leq 0.004^a$

^aPossible interference from ^{244}Cm .

The curium and plutonium content of SRL-31 was determined by radiochemical analysis for ^{244}Cm and ^{240}Pu , and the total element weight was calculated by use of the isotopic abundances given in Table 29. The results of the assay are shown in Table 30.

Table 30. Curium and Plutonium Content in SRL-31 Oxide

Sample No.	Weight (mg)	Curium (mg/g)	Plutonium (mg/g)	Cm_2O_3 (mg/g)	PuO_2 (mg/g)
Cm-31-4C	19.3	753	78	827	88
Cm-31-5C	20.0	807	70	888	79
Cm-31-6C	13.9	839	73	922	83
Average		800	74	879	84
Adjusted average ^a		840		923	

^aBased on a calorimetric value of 2.24 W/g of Cm_2O_3 product.

The radioactive impurities were determined by standard germanium crystal gamma spectrometry and are listed in Table 31.

Table 31. Radioactive Impurities in SRL-31 Oxide

Nuclide	Curies/g
Ruthenium-103	$\leq 9 \times 10^{-6}$
Ruthenium-106	$\leq 3 \times 10^{-5}$
Cesium-134	$\leq 3 \times 10^{-6}$
Cesium-137	$\leq 5 \times 10^{-6}$
Cerium-144	$\leq 4 \times 10^{-4}$
Praseodymium-144	$\leq 4 \times 10^{-4}$
Zirconium-95	$\leq 1 \times 10^{-5}$
Niobium-95	$\leq 4 \times 10^{-6}$
Europium-154	$\leq 1 \times 10^{-5}$
Americium-243	9×10^{-3}

The non-radioactive impurities were determined by spark source mass spectrometry and are listed in Table 32. The weight of these impurities in the form of oxides is ~15 mg per gram of sample. The principal individual impurities are 10.9 mg of AmO_2 and 1.8 mg of Fe_2O_3 per gram of sample.

Table 32. Impurities in Batch SRL-31 Curium Oxide

Element	Wt (ppm of Cm)	Element	Wt (ppm of Cm)
Aluminum	20	Molybdenum	200
Arsenic	<10	Sodium	200
Boron	<10	Nickel	100
Barium	<10	Lead	100
Calcium	20	Platinum	100
Cobalt	<10	Silicon	100
Chromium	100	Tantalum	150
Copper	30	Titanium	<100
Iron	1,500	Zinc	<20
Potassium	10	Zirconium	<500
Magnesium	<10	Americium	12,000
Manganese	30	Rare Earths	300

In summary, the composition of SRL-31 oxide is:

<u>Material</u>	<u>mg/g</u>	<u>Percent</u>
Cm ₂ O ₃	923	90.3
PuO ₂	84	8.2
Impurities	~15	1.5

Curium Oxide Purification (*T. A. Butler and C. L. Ottinger*)

Two batches (72-Cm-3 and 72-Cm-4) of impure ²⁴⁴Cm oxide recovered from the Kilowatt Heat Source Test were reprocessed by the ORNL TRU facility. The principal contaminants were ²⁴⁰PuO₂ from alpha decay of ²⁴⁴Cm and tungsten from the milling operation during recovery of the fuel from the heat source test capsule. Processing steps used by the TRU facility in achieving a high degree of purification included: (1) dissolution of the curium oxide in nitric acid, (2) separation from tungsten by decantation and filtration, (3) removal of ²⁴⁰Pu using a Pubex (HDEHP) batch solvent extraction, (4) purification from other impurities using two cycles of oxalate precipitation, and (5) preparation of curium oxide by calcination of the oxalate in air for 2 hr at 700°C.

Five fractions of purified curium oxide containing a total of 77.0 g of ²⁴⁴Cm were received from the TRU facility. These represent the yields from two purification cycles made on residues containing a total of 88.5 g of ²⁴⁴Cm. Purification from plutonium and other impurities was excellent. The purified material contained an average of only 0.15 wt % plutonium. Americium, which was not separated, is the major impurity at 1.2 wt %; all other detected contaminants total less than 0.2%.

The purified product from batch 72-Cm-4 was returned in three lots, SR Cm-30, -31, and -32. Analyses were made on a composite sample prepared from grab samples of each lot. The assay data are given in Tables 33, 34, and 35.

Table 33. Curium Oxide Product Weight and ^{244}Cm Content

Lot Number	Weight (g)	^{244}Cm by Calorimetry (g) ^a
SR Cm-30	14.85	12.19
SR Cm-31	19.04	15.47
SR Cm-32	<u>15.50</u>	<u>12.74</u>
Total	49.39	40.40

^aDate: July 27, 1973.

Table 34. Isotopic Analysis of Composite SR Cm-30, -31, -32

Curium Mass Number	Isotopic Abundance (atom %) ^a
244	94.21
245	0.874
246	4.79
247	0.080
248	0.048

^aDate: July 13, 1973.

Table 35. Impurities in Composite SR Cm-30, -31, -32^a

Impurity	Assumed Oxidized Form	Product (ppm) ^b	Impurity	Assumed Oxidized Form	Product (ppm) ^b
Al	Al_2O_3	8	P	P_2O_5	11
As	As_2O_3	4	Pb	PbO_2	58
B	B_2O_3	16	S	SO_3	125
Bi	Bi_2O_3	8	Si	SiO_2	<13
Ca	CaO	7	Ta	Ta_2O_5	25
Cl	Cl	50	Ti	TiO_2	<2
Co	CoO	1	V	V_2O_5	<2
Cr	CrO_3	4	W	WO_3	126
Cu	CuO	11	Zn	ZnO	10
F	F	10	Zr	ZrO_2	135
Fe	Fe_2O_3	11	Y	Y_2O_3	5
K	K_2O	4	RE's	$(\text{RE})_2\text{O}_3$	769
Li ^c	Li_2O	<4	$^{240}\text{Pu}^d$	PuO_2	1,877
Mg	MgO	<3	$^{243}\text{Am}^d$	AmO_2	12,240 ^e
Mn	MnO_2	<1	$^{252}\text{Cf}^d$	Cf_2O_3	<1
Mo	MoO_3	<2			
Na	Na_2O	<13	Total		15,557
Ni	NiO	6			

^aAnalyses were by spark source mass spectrometry except where indicated.

^bParts of impurity oxide per million parts of total curium metal.

^cAnalyzed by flame photometry.

^dRadiochemical analysis.

^eAnalysis by fast neutron counting indicated that the product contained 0.07 ± 0.1 ppm ^{252}Cf more than the feed.

The purified product from batch 72-Cm-3 was returned in two lots, SR Cm-33 and -34. Analyses were made on a composite sample prepared from grab samples of each lot. The assay data are given in Tables 36, 37, and 38.

Table 36. Curium Oxide Product Weight and ^{244}Cm Content

Lot Number	Weight (g)	^{244}Cm by Calorimetry (g) ^a
SR Cm-33	26.82	22.12
SR Cm-34	<u>17.61</u>	<u>14.52</u>
Total	44.43	36.64

^aDate: August 13, 1973.

Table 37. Isotopic Analysis of Composite SR Cm-33, -34

Curium Mass Number	Isotopic Abundance (atom %) ^a
244	94.18
245	0.94
246	4.75
247	0.083
248	0.047

^aDate: August 10, 1973.

Table 38. Impurities in Composite SR Cm-33, -34^a

Impurity	Assumed Oxidized Form	Product (ppm) ^b	Impurity	Assumed Oxidized Form	Product (ppm) ^b
Al	Al ₂ O ₃	19	Ni	NiO	25
As	As ₂ O ₃	11	P	P ₂ O ₅	69
B	B ₂ O ₃	97	Pb	PbO ₂	46
Ba	BaO	<1	S	SO ₃	749
Bi	Bi ₂ O ₃	11	Si	SiO ₂	642
Ca	CaO	70	Ta	Ta ₂ O ₅	102
Cl	Cl	60	Ti	TiO ₂	<9
Co	CoO	<1	V	V ₂ O ₅	2
Cr	CrO ₃	19	W	WO ₃	63
Cu	CuO	8	Zn	ZnO	6
F	F	70	Zr	ZrO ₂	270
Fe	Fe ₂ O ₃	57	RE's	(RE) ₂ O ₃	470
K	K ₂ O	12	$^{240}\text{Pu}^{\text{c}}$	PuO ₂	1,174
Li ^d	Li ₂ O	<5	$^{243}\text{Am}^{\text{c}}$	AmO ₂	11,448
Mg	MgO	50	$^{252}\text{Cf}^{\text{c}}$	Cf ₂ O ₃	<1 ^e
Mn	MnO ₂	6			
Mo	MoO ₃	<5	Total		16,115
Na	Na ₂ O	539			

^aAnalyses were by spark source mass spectrometry except where indicated.

^bParts of impurity oxide per million parts of total curium metal.

^cRadiochemical analysis.

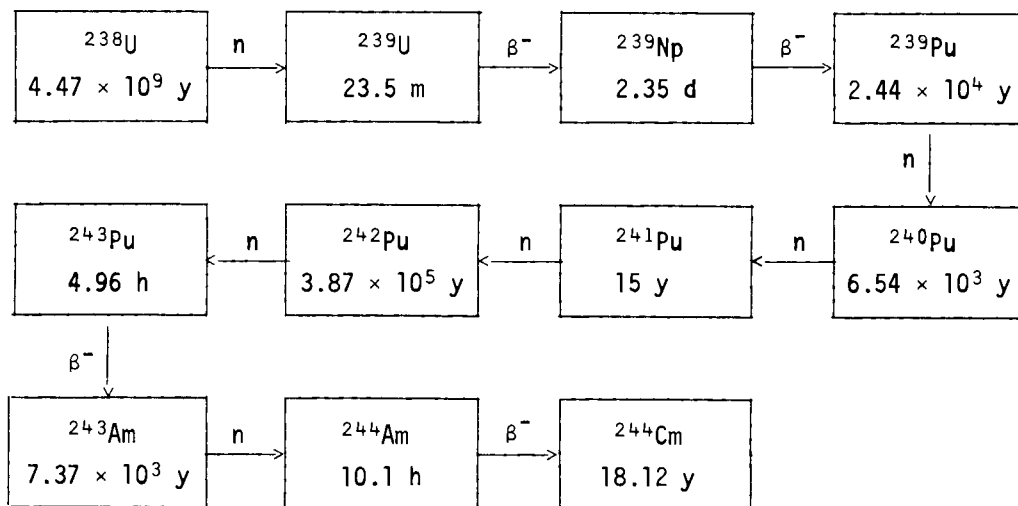
^dAnalyzed by flame photometry.

^eAnalysis by fast neutron counting indicated that the product contained no more ^{252}Cf than the feed material.

Curium From Power Reactor Fuels (*T. A. Butler*)

The future source of ^{244}Cm in quantity is expected to derive from the reprocessing of power reactor fuels. A study was begun to examine some of the factors which influence the amount of ^{244}Cm produced in the reactor fuels and to estimate future quantities available from this source for isotopic power fuels. In this study, assistance is provided by C. W. Kee, Engineering Coordination and Analysis Section, ORNL Chemical Technology Division, and of F. T. Binford, Development Department, ORNL Operations Division. Computer calculations and interpretation of the data are supplied by C. W. Kee.

The nuclear reactions which lead to the formation of ^{244}Cm in uranium-fueled reactors are as follows:



In a previous report⁵ the yield of ^{244}Cm from reference PWR reactors was given as a function of burnup (MWD/MT) for both enriched ^{235}U and plutonium recycle fueled reactors for specified operating conditions. A large increase in ^{244}Cm yield from plutonium recycle fuel is evident, but significant quantities of these fuels are not expected to be available for a decade or so.

The production rate of ^{244}Cm in enriched uranium fuels is dependent on the total fluence (neutron flux \times time) rather than on burnup alone. The neutron flux required to maintain constant reactor power levels is greater for less enriched fuels while the amount of ^{238}U present is about the same. The rate of neutron captures leading eventually to ^{244}Cm is therefore increased. To demonstrate this effect, ORIGEN⁹ calculations were made for PWR reference reactors operating at a power of 30 MW/MT and fueled with 1.5, 2.0, 2.5, 2.8, and 3.3% ^{235}U enrichments.

In these calculations, it was assumed that the neutron energy spectrum is the same in all cases. This is approximately true since most of the fissions are from ^{235}U . Small differences occur because of the buildup

of a varying amount of plutonium during the life of the reactor fuel; however, this should not introduce large errors in the calculated yields of ^{244}Cm . The results of the calculations are given in Tables 39 and 40 and Fig. 5. Figure 5 is a graphic display of values given in Table 40.

Table 39. Average Neutron Flux as a Function of Fuel Enrichment

Reactor Power: 30 MW/MT	
Fuel Burnup: 33 GWD/MT	
^{235}U Enrichment (%)	Average Neutron Flux ($\text{n}/\text{cm}^2 \cdot \text{sec}$)
1.5	4.25×10^{13}
2.0	3.83×10^{13}
2.5	3.45×10^{13}
2.8	3.24×10^{13}
3.3	2.92×10^{13}

Table 40. Influence of ^{235}U Enrichment on ^{244}Cm Yield in Power Reactor Fuel

Burnup [GWD/MT(U)]	^{244}Cm Yield [g/MT(U)]				
	^{235}U Enrichment (%)				
	1.5	2.0	2.5	2.8	3.3
3.3	0.004	0.001	0.0003	0.0002	.00008
6.6	0.11	0.038	0.015	0.009	0.004
9.9	0.75	0.31	0.14	0.09	0.04
13.2	2.9	1.3	0.63	0.42	0.22
16.5	7.8	3.9	2.0	1.4	0.74
19.8	17.3	9.3	5.1	3.6	2.0
23.1	32.9	19.1	11.1	8.0	4.7
26.4	56.9	35.0	21.2	15.7	9.5
29.7	89.8	58.1	37.1	28.1	17.6
33.0	133.0	89.8	59.8	46.4	30.3

The potential supply of ^{244}Cm from power reactor fuel reprocessing for isotopic power fuel applications is projected to be more than adequate for anticipated needs.¹⁰

Variations in the isotopic composition of curium will occur, depending on the type and operating parameters of power reactors, which will be important to the chemical recovery process and characterization of the

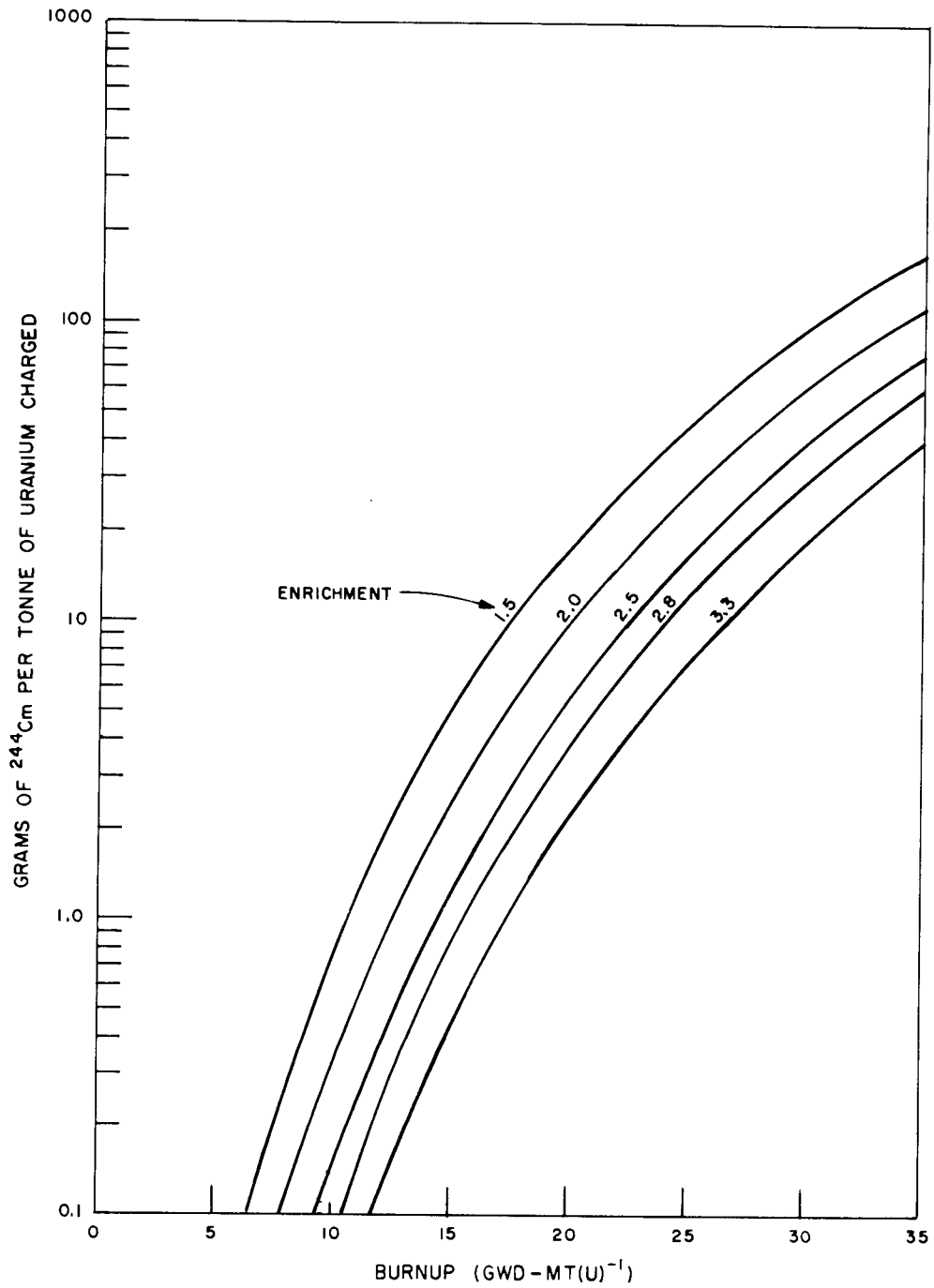


Fig. 5. Influence of Enrichment on Curium Production.

curium fuel form. The characterization of $^{244}\text{Cm}_2\text{O}_3$ fuel to date has been done for the most part on material produced by irradiation of plutonium isotopes in the USAEC Savannah River reactors. A typical isotopic composition of this material after a decay period of five years following reactor discharge is as follows:

<u>Curium Mass No.</u>	<u>Atom %</u>
243	0.025
244	94.46
245	0.828
246	4.57
247	0.075
248	0.043

The most significant difference in the isotopic abundance of curium from power reactor fuels versus Savannah River product is an increase in the abundance of the ^{243}Cm and ^{245}Cm isotopes. The ^{244}Cm content will decrease by a few percent and thus lower the specific power of the fuel. Both ^{243}Cm and ^{245}Cm have high fission cross sections, and thus evaluation will be required of possible criticality problems in aqueous processing of curium concentrates and in design of heat sources. In addition, ^{243}Cm has gamma-ray emissions of 0.211 (5.6%), 0.228 (7.3%), and 0.278 (11.2%) MeV which influence shielding considerations.

Very little measured data are available on the isotopic composition of curium from power reactor fuels. Assay of curium recovered from the normal uranium blanket of the Shippingport reactor after about a 3-year decay period showed the following isotopic composition.¹¹

<u>Curium Mass No.</u>	<u>Atom %</u>
243	1.53
244	93.64
245	4.05
246	0.762
247	0.094
248	0.002

In Table 41 the abundances of the four principal curium isotopes following a 5-year decay period are shown as calculated by the ORIGEN code for various types of reference power reactors. The calculations are useful in indicating the range of isotopic concentration variations that may be anticipated until more measured data become available.

Table 41. Isotopic Abundance of Curium Isotopes
for Various Power Reactor Fuels

Reactor Type	Burnup (GWD)	Isotopic Abundance (atom %)			
		^{243}Cm	^{244}Cm	^{245}Cm	^{246}Cm
PWR (3.3% ^{235}U)	33	0.27	91.8	7.1	0.8
HTGR (Th + U)	94	0.07	91.4	6.3	2.2
PWR (U + Pu)	33	0.05	86.5	12.2	1.3
AI - LMFBR	37	5.54	92.7	2.0	0.04
GE - LMFBR	42	5.53	91.3	3.1	0.1

Curium Source Fabrication Facility Operation

(C. L. Ottinger)

Equipment repairs, recalibrations, and necessary replacements were made in preparation for experimental work. A considerable amount of solid waste resulting from previous operations was discarded. Two batches of ^{244}Cm residues resulting from the Kilowatt Test Source defueling were transferred to the TRU facility for reprocessing. The reprocessed ^{244}Cm was returned in five batches, two of which were opened and used for experiments.

Operations in support of ^{244}Cm work included preparation of $^{244}\text{Cm}_2\text{O}_3$ pellets for the ceramic compatibility tests, remeasurement of the heat output of the neutron test source, and transfers of pellets to the leach-rate study facility. Experiments done at the CSFF are described under "Dimensional Stability," "Reaction of Cm_2O_3 With Dry Air," and " $^{244}\text{Cm}_2\text{O}_3$ Radiation Measurements."

REFERENCES

1. Eugene Lamb, *ORNL Isotopic Power Fuels Quarterly Report for Period Ending December 31, 1971*, ORNL-4774, Oak Ridge National Laboratory.
2. J. H. Hildebrand and R. L. Scott, *The Solubility of Non-electrolytes*, Reinhold Publishing Corporation, New York, 1950, pp. 198-209 and 320-347.
3. Alvin Glassner, *The Thermochemical Properties of the Oxides, Fluorides, and Chlorides to 2500°K*, ANL-5750, Argonne National Laboratory (1957).
4. F. L. Oetting, "The Chemical Thermodynamic Properties of Plutonium Compounds," *Chem. Rev.* 67, 261-97 (June 1967).
5. Eugene Lamb, *ORNL Isotopic Power Fuels Quarterly Report for Period Ending June 30, 1973*, ORNL-4917, Oak Ridge National Laboratory.
6. R. Stull and H. Prophet (eds.), *JANAF Thermochemical Tables*, 2nd Ed., NSRDS-NBS-37, Office of Standard Reference Data, National Bureau of Standards (1971).
7. R. A. Kent, *Thermodynamic Analyses of MHW Space Electric Power Generator*, LA-5202 MS, Los Alamos Scientific Laboratory (March 1973).
8. D. H. Stoddard, *Radiation Properties of ^{244}Cm Produced for Isotopic Power Generators*, DP-939, Savannah River Laboratory (November 1964).
9. M. J. Bell, *ORIGEN - The ORNL Isotope Generation and Depletion Code*, ORNL-4628, Oak Ridge National Laboratory (May 1973).
10. Eugene Lamb, D. G. Albertson, and Paul E. Brown, "The Availability and Cost of Curium-244 From Power Reactor Fuel Reprocessing Wastes," presented at *Intersociety Energy Conversion Conference, Philadelphia, PA, August 1973*.
11. Private communication, J. E. Bigelow, Oak Ridge National Laboratory, September 1973.

INTERNAL DISTRIBUTION

- | | | | |
|-------|-------------------------------|-----|----------------|
| 1-3. | Central Research Library | 38. | R. F. Hibbs |
| 4. | ORNL — Y-12 Technical Library | 39. | M. R. Hill |
| | Document Reference Section | 40. | H. Inouye |
| 5-24. | Laboratory Records Department | 41. | E. Lamb |
| 25. | Laboratory Records, ORNL RC | 42. | R. E. Leuze |
| 26. | G. M. Adamson, Jr. | 43. | H. C. McCurdy |
| 27. | P. Angelini | 44. | C. L. Ottinger |
| 28. | N. C. Bradley | 45. | J. C. Posey |
| 29. | T. A. Butler | 46. | A. F. Rupp |
| 30. | C. E. Clifford | 47. | R. W. Schaich |
| 31. | F. L. Culler | 48. | M. J. Skinner |
| 32. | J. E. Cunningham | 49. | D. A. Sundberg |
| 33. | J. R. DiStefano | 50. | D. B. Trauger |
| 34. | R. G. Donnelly | 51. | A. M. Weinberg |
| 35. | D. E. Ferguson | 52. | J. R. Weir |
| 36. | J. H. Gillette | 53. | A. Zucker |
| 37. | K. W. Haff | | |

EXTERNAL DISTRIBUTION

54. R. D. Baker, Los Alamos Scientific Laboratory
55. F. P. Baranowski, Division of Production & Materials Management, AEC
56. M. Bell, TRW Systems
57. Linda Benker, Thermo Electron Corporation
58. R. F. Borlick, Division of Production & Materials Management, AEC
59. H. C. Carney, Jr., Gulf Energy and Environmental Services
60. R. T. Carpenter, Division of Space Nuclear Systems, AEC
61. W. T. Cave, Mound Laboratory
62. Commander, Naval Undersea Research and Development Center
63. G. R. Crane, Headquarters AFSC (XRTS), Andrews Air Force Base
64. G. P. Dix, Division of Space Nuclear Systems, AEC
65. R. English, NASA, Lewis Research Center
66. T. P. Fleming, Naval Facilities Engineering Command
67. R. K. Flitcraft, Mound Laboratory
- 68-70. E. E. Fowler, Division of Applied Technology, AEC
71. L. Frank, Weiner Associates, Inc.
72. A. G. Fremling, AEC-Richland Operations Office
73. D. S. Gabriel, Division of Space Nuclear Systems, AEC
74. N. Goldenberg, Division of Space Nuclear Systems, AEC
75. M. Goldman, Division of Biomedical & Environmental Research, AEC
76. R. C. Hamilton, IDA — Room 19, 400 Army-Navy Drive, Arlington, VA
77. W. J. Haubach, Division of Physical Research, AEC
78. M. G. Hegarty, Radio Corporation of America
79. T. B. Hindman, AEC-Savannah River Operations Office
80. R. E. Hopkins, U.S. Army Mobility Equipment R&D Center
81. Ian Jones, TRW Systems

82. T. B. Kerr, NASA Headquarters
83. F. E. Kruesi, Savannah River Laboratory
84. J. A. Lieberman, Division of Reactor Research and Development
85. G. Linkous, Teledyne-Isotopes, Inc.
86. W. A. McDonald, Teledyne-Isotopes, Inc.
87. T. A. Nemzek, Division of Reactor Research and Development, AEC
88. G. A. Newby, Division of Space Nuclear Systems, AEC
89. W. G. Parker, Westinghouse Astronuclear Laboratory
90. F. K. Pittman, Division of Waste Management & Transportation, AEC
91. G. B. Pleat, Division of Production & Materials Management, AEC
92. R. W. Ramsey, Jr., Division of Waste Management & Transportation, AEC
93. R. Schafer, General Electric Company
94. P. K. Smith, E. I. duPont-Savannah River Laboratory
95. J. M. Teem, Division of Physical Research, AEC
96. H. H. Van Tuyl, Pacific Northwest Laboratories
97. R. L. Wainwright, Dayton Area Office, AEC
98. J. L. Womack, E. I. duPont-Savannah River Plant
99. AEC, Richland Operations Office
100. AEC, Savannah River Operations Office
101. General Electric Company, MSD, AEC
102. General Electric Company, VNC, AEC
103. NASA, Goddard Space Flight Center
104. NASA, Langley Research Center
105. NASA, Manned Spacecraft Center
106. NASA, Marshall Space Flight Center
107. Navy Space Systems Activity
108. Teledyne-Isotopes, Inc., Timonium, MD
109. Research and Technical Support Division, AEC, ORO
110. Patent Office, AEC, ORO
- 111-277. Given distribution as shown in TID-4500 under Nuclear Propulsion Systems and Aerospace Safety category (25 copies - NTIS)